Generalized Riemann problem for dispersive equations

Sergey Gavrilyuk, Boniface Nkonga, Keh-Ming Shyue, Lev Truskinovsky

Generalized Riemann problem for dispersive equations

Sergey Gavrilyuk*, Boniface Nkonga †, Keh-Ming Shyue ‡, Lev Truskinovsky §

December 17, 2018

Abstract

We study the inertia type regularization of equations for barotropic fluids. This regularization is formally obtained as the Euler-Lagrange equations for a Lagrangian containing terms which are quadratic with respect to the material derivative of density. Such a regularization arises, in particular, in the modeling of waves in bubbly fluids as well as in the theory of water waves (Serre-Green-Naghdi equations).

We show that such terms are not always regularizing. The solution can develop shocks even in the presence of dispersive terms. In particular, we found such a shock solution relating a constant state with a periodic wave train. The shock speed coincides necessarily with the velocity of the corresponding wave train. The associated Rankine-Hugoniot relations correspond to Whitham's equations (modulation equations) of the regularized system.

The numerical evidence of the existence of such shocks is demonstrated. To this aim, a robust high-order accurate numerical has been designed based on an appropriate operator splitting of the governing equations. In particular, it has been shown that such waves can dynamically be formed. Also, when such a wave is used for initial data, it is not destroyed by small perturbations. This proves a certain stability of these waves.

1 Introduction

Classical mechanics operates often with the following barotropic (isentropic or isothermic) model of compressible flows :

$$\rho_t + (\rho\, u)_x = 0, \quad (\rho u)_t + (\rho\, u^2 + p(\rho))_x = 0. \tag{1}$$

Here t is the time, x is the space coordinate, ρ is the fluid density, u is the velocity, $p(\rho) = \rho^2 \dfrac{\partial \varepsilon}{\partial \rho}$ is the pressure, and $\varepsilon(\rho)$ is a given specific energy. An analogous system appears also in the study of the wave propagation in shallow water (Saint-Venant equations). The Lagrangian for this system is given by

$$L = \rho \left(\frac{u^2}{2} - \varepsilon(\rho) \right).$$

*Aix Marseille Univ, CNRS, IUSTI, UMR 7343, Marseille, France, sergey.gavrilyuk@univ-amu.fr

†Université de Nice Sophia-Antipolis, CNRS UMR 7351, Laboratoire J.A.Dieudonné, Parc Valrose, 06108 NICE Cedex 2 France, Boniface.Nkonga@unice.fr

‡Institute of Mathematical Sciences, National Taiwan University, Taipei 106, Taiwan, shyue@ntu.edu.tw

§ESPCI ParisTech, Paris, France, lev.truskinovsky@espci.fr

The Noether theorem implies the energy conservation law

$$\left(\rho\left(\frac{u^2}{2}+\varepsilon(\rho)\right)\right)_t+\left(\rho u\left(\frac{u^2}{2}+\varepsilon(\rho)\right)+pu\right)_x=0,$$

and the Bernoulli law

$$u_t+\left(\frac{u^2}{2}+\varepsilon+\frac{p}{\rho}\right)_x=0.$$

This model conserves the energy while the solution stays smooth. As soon as singularities form (shocks, for example) the energy starts to dissipate. Indeed, the Rankine-Hugoniot relations coming from the mass and momentum equations are :

$$[\rho(u-D)]=0,$$

$$\left[\rho(u-D)^2+p\right]=0.$$

Here D is the shock velocity, and for any function f we have denoted $[f]=f^+-f^-$ where the superscripts $\pm$ denote the limit values of f at the shock. The two other conservation laws can be taken as the entropy inequality. The energy conservation law and Bernoulli conservation law give the same jump relations:

$$\left[(u-D)^2+\varepsilon+\frac{p}{\rho}\right]=0. \tag{2}$$

We see that the energy conservation law (as well as the Bernoulli conservation law) are incompatible with the conservation of momentum. To handle and to understand this phenomena, there are three different approaches. One is to phenomenologically assume that there is a dissipation associated with singularities, second is to regularize the equations by adding the viscosity type dissipation, and third is to regularize the equations by non-dissipative way (dispersive). The disadvantage of the first approaches is that the dissipation is brought into conservative systems 'ad hoc' ('by hands'). Also, purely dissipative regularization does not predict an overshooting of shock waves as usually happens for the wave propagating in dispersive systems. In order to understand the transition from the non-dissipative to dissipative system we will use the dispersive regularization, because it preserves the non-dissipative structure of original system.

Two types of dispersion can be put into the system. The first is adding higher space derivatives of the density (*capillarity type regularization*), and the second one is adding the material time derivatives of density (*inertia type regularization*).

Such a dispersive regularization can be presented in the following simple form using the mass Lagrangian coordinate

$$q=\int_0^Y \rho_0(s)ds, \tag{3}$$

where Y is the Lagrangian coordinate, and $\rho_0(Y)$ is the initial density. Consider the following modified Lagrangian :

$$L=\int_{-\infty}^{+\infty}\left(\frac{u^2}{2}-\tilde{e}(\tau,\tau_t,\tau_q)\right)dq, \tag{4}$$

where $\tilde{e}(\tau,\tau_t,\tau_q)$ is a given potential satisfying the natural relation

$$\tilde{e}(\tau,0,0)=e(\tau)=\varepsilon\left(\frac{1}{\tau}\right). \tag{5}$$

Then, the corresponding Euler-Lagrange equations can be written in the form :

$$\tau_t - u_q = 0, \quad u_t + p_q = 0, \tag{6}$$

where

$$\tau = \frac{1}{\rho}, \quad p = -\frac{\delta \tilde{e}}{\delta \tau} = -\left(\frac{\partial \tilde{e}}{\partial \tau} - \frac{\partial}{\partial t}\left(\frac{\partial \tilde{e}}{\partial \tau_t}\right) - \frac{\partial}{\partial q}\left(\frac{\partial \tilde{e}}{\partial \tau_q}\right)\right). \tag{7}$$

When one of the partial derivatives, τ_t or τ_q, is absent in the general expression of $\tilde{e}$, we call the case $\tilde{e} = \tilde{e}(\tau, \tau_q)$ ($\tilde{e} = \tilde{e}(\tau, \tau_t)$) *capillarity type* (*inertia type*) regularization, respectively.

As for the barotropic flows, due to the Noether theorem, system (6), (7) admits two conservation laws. One of them is the energy equation :

$$\left(\frac{u^2}{2} + \varepsilon\right)_t + \left(pu - \tau_t \frac{\partial \tilde{e}}{\partial \tau_q}\right)_q = 0, \quad \varepsilon = \tilde{e} - \tau_t \frac{\partial \tilde{e}}{\partial \tau_t}. \tag{8}$$

while the other one is the Bernoulli conservation law :

$$\left(\tau u - \tau_q \frac{\partial \tilde{e}}{\partial \tau_t}\right)_t - \left(\frac{u^2}{2} - \tau p + \tau_q \frac{\partial \tilde{e}}{\partial \tau_q} - \tilde{e}\right)_q = 0. \tag{9}$$

Both types of dispersion naturally appear in different fields of physics. The capillarity type regularization appears in compressible fluid dynamics (through numerical methods) [33], [23]), in the description of moving phase interfaces [37], [51], [48], [50], [44], [12], critical nuclei problems [49], in quantum physics [24], [8] etc.

The inertia type regularization appears in the theory of wave propagation in solids [38] and fluids containing gas bubbles [11], [13], [15], in asymptotic theories of water waves [34], [40], [46], [16], [17]. Finally, both types of regularization can appear (cf. [5], [4] in the theory of long water waves).

In this paper we will concentrate on the inertia type regularization. In particular, we will show that this type of dispersion does not always allow us to regularize the solutions of the governing equations: they continue to develop the shocks as usually happens for hyperbolic equations. The relation between such shocks and the shock solution of the corresponding Whitham system [52] is found. We have also to mention here the recent results in [9] where the shock solution to the Benjamin-Bona-Mahony (BBM) equation was found. This solution was at the same time a weak solution to the Hopf equation which is a hyperbolic part of the BBM equation. This results is quite unexpected, because the word 'regularisation' becomes senseless.

To be specific, we will concentrate on the Serre-Green-Naghdi (SGN) equations describing long water waves. However, our results are quite generic : one can expect the existence of discontinuous solutions for any inertia type regularization.

SGN equations can be written in the Eulerian coordinates in the form [40], [46], [16], [17] :

$$h_t + (hu)_x = 0, \quad (hu) + (hu^2 + p)_x = 0, \tag{10}$$

where

$$p = \frac{gh^2}{2} + \frac{1}{3}h^2 \frac{D^2 h}{Dt^2}, \quad \frac{D^2}{Dt^2} = \frac{D}{Dt}\,\frac{D}{Dt}, \quad \frac{D}{Dt} = \frac{\partial}{\partial t} + u\,\frac{\partial}{\partial x}.$$

Here h is the fluid depth (it can be seen as the analogue of ρ), u is the averaged over the fluid depth velocity, p is the integrated over the fluid depth pressure. If l is a characteristic wave length,

and h_0 is the mean water depth, we define the dimensionless small parameter $\beta = h_0^2/l^2$. The SGN equations are obtained by depth-averaging the Euler system and keeping in the resulting set of equations only first order terms in β without making any assumptions on the amplitude of the waves.

A mathematical justification of this model and some related systems can be found in [27], [31], [39]. Recent years have seen increased activity in both the study of qualitative properties of the solutions to the SGN system and in the development of numerical discretization techniques [30], [32], [10].

Note that when higher-order terms in (10) are discarded, the system reduces to the classical Saint-Venant equations. The Lagrangian for (10) is given by [34], [13] :

$$L = h\left(\frac{u^2}{2} + \frac{1}{6}\left(\frac{Dh}{Dt}\right)^2 - \frac{gh}{2}\right).$$

In the mass Lagrangian coordinates, the system is of the form (6)–(7) with the potential $\tilde{e}$ given by the following expression :

$$\tilde{e}(\tau, \tau_t) = \frac{g}{2\tau} - \frac{1}{6}\left(\frac{\partial}{\partial t}\left(\frac{1}{\tau}\right)\right)^2 = \frac{g}{2\tau} - \frac{\tau_t^2}{6\tau^4}, \quad \tau = \frac{1}{h}.$$

In the Eulerian coordinates, the energy conservation law is :

$$\left(h\left(\frac{u^2}{2} + \varepsilon\right)\right)_t + \left(hu\left(\frac{u^2}{2} + \varepsilon\right) + pu\right)_x = 0, \tag{11}$$

with

$$\varepsilon = \frac{1}{6}\left(\frac{Dh}{Dt}\right)^2 + \frac{gh}{2}.$$

The Bernoulli conservation law for variable $K = u - \frac{1}{3h}\left(h^3 u_x\right)_x$ (which is the tangent component of fluid velocity at the free surface [14]) is :

$$K_t + \left(Ku + gh - \frac{u^2}{2} - \frac{1}{2}h_x^2 u^2\right)_x = 0. \tag{12}$$

2 Riemann problem for dispersive systems of equations

The solution of the classical Riemann problem (the Cauchy problem with discontinuous piece-wise constant initial data) is well studied for hyperbolic system of equations (cf. [41]). For dispersive equations (or dispersive systems of equations) this problem is always a subject of intensive research. Much progress has been done for the Riemann problem for integrable equations [19], [6], [20], [35], and much less for non-integrable equations (cf. [7], [32], [1]) (cf. a recent review article on this subject [8]).

In particular, for SGN equations (10) the Riemann problem is formulated as follows :

$$\begin{pmatrix} h(0,x) \\ u(0,x) \end{pmatrix} = \begin{cases} \begin{pmatrix} h_L \\ u_L \end{pmatrix}, \text{ if } \quad x < 0, \\ \begin{pmatrix} h_R \\ u_R \end{pmatrix}, \text{ if } \quad x > 0. \end{cases}$$

where $h_{L,R} > 0$ and $u_{L,R}$ are constants. The Riemann problem for the SGN equations was mainly studied in the case of a dam-break problem where $u_{L,R} = 0$ (cf. [7] (analytical and numerical study) and [32], [36] (numerical study)).

A further natural step would be to consider the following *generalized Riemann problem*:

$$\begin{pmatrix} h(0,x) \\ u(0,x) \end{pmatrix} = \begin{cases} \begin{pmatrix} h_L(x) \\ u_L(x) \end{pmatrix}, \text{if} \quad x < 0, \\ \begin{pmatrix} h_R(x) \\ u_R(x) \end{pmatrix}, \text{if} \quad x > 0. \end{cases}$$

Here $h_{L,R}(x)$ and $u_{L,R}(x)$ are periodic travelling wave solutions to the SGN system. For example, for the 'generalized' dam break problem, the one of the states (left or right) can be interpreted as a periodic wave train created by the wind, while the other state where the fluid has a lower level corresponds, for example, to a constant downstream state. Such a generalized Riemann problem corresponds to a non-linear interaction of two periodic wave trains (or a periodic wave train with a constant state) having different wave characteristics.

The role of numerical modeling in the study of such a problem becomes a determining factor.

3 Travelling wave solutions for SGN equations

This study will be devoted to the search of traveling waves for the SGN equations (10). Such a study can also be found in the literature (cf. [7]). We present it for completeness. We look for particular solutions $(h(\xi), u(\xi))$, where $\xi = x - Dt$ and D is a constant. It follows from the first equation:

$$-Dh' + (hu)' = 0,$$

where the derivation is performed with respect to the variable ξ. This is more conveniently written as:

$$(-Dh + hu)' = 0.$$

This can be integrated once to yield to :

$$h(u - D) = const \stackrel{def}{=} m. \tag{13}$$

We pass to the second equation and we get :

$$(hu(u - D) + p)' = 0.$$

From (13) it follows:

$$(mu + p)' = 0.$$

We substract the constant mD inside the brackets, which does not change the value of the expression. This unables us to write:

$$(m(u - D) + p)' = 0.$$

Using again (13), we can conclude that

$$p + \frac{m^2}{h} = const \stackrel{def}{=} i. \tag{14}$$

We need to compute the expression of the second derivative $\dfrac{D^2h}{Dt^2}$ in terms of ξ. To do that we pass to the following calculation. The material derivative reads :

$$\frac{Dh}{Dt} = h_t + uh_x = h'(u - D)$$

in terms of the new variables. Thus, making use of (13), we have:

$$\frac{D^2h}{Dt^2} = \frac{D}{Dt}\left(\frac{Dh}{Dt}\right) = \left(h'(u-D)\right)'(u-D) = \left(\frac{h'}{h}m\right)'\frac{m}{h} = \frac{m^2}{h}\left(\frac{h'}{h}\right)'.$$

Equation (14) now becomes

$$\frac{1}{2}gh^2 + \frac{1}{3}m^2h\left(\frac{h'}{h}\right)' + \frac{m^2}{h} = i.$$

By multiplying both sides of the equation by $h'/(m^2h^2)$ one obtains :

$$\frac{1}{6}\left(\left(\frac{h'}{h}\right)^2\right)' + \frac{g}{2m^2}h' + \frac{1}{h^3}h' - \frac{i}{m^2h^2}h' = 0.$$

By multiplication of both sides of the equation by h'/h, we can at once obtain the integral:

$$\frac{1}{6}\left(\frac{h'}{h}\right)^2 + \frac{g}{2m^2}h - \frac{1}{2h^2} + \frac{i}{m^2h} = const \stackrel{def}{=} e, \tag{15}$$

and this can be recast as:

$$(h')^2 = F(h), \tag{16}$$

where $F(h)$ is the following third order degree polynomial on h :

$$F(h) = -\frac{3g}{m^2}h^3 + 6eh^2 - \frac{6i}{m^2}h + 3.$$

Equation (16) can also be obtained directly from (11) or (12). An inequality to be imposed is $F(h) \geq 0$. We write $F(h)$ in the form:

$$F(h) = \frac{3g}{m^2}P(h), \quad P(h) = (h - h_0)(h - h_1)(h_2 - h),$$

where

$$0 < h_0 \leq h_1 < h_2 < \infty.$$

Expanding the expression for $P(h)$ we obtain:

$$m^2 = gh_0h_1h_2, \quad i = \frac{g}{2}(h_0h_1 + h_0h_2 + h_1h_2), \quad \text{and} \quad e = \frac{h_0 + h_1 + h_2}{2h_0h_1h_2}.$$

The periodic solution corresponds to $h_0 < h_1 < h_2$, it oscillates between h_1 and h_2 and is given by the formula :

$$h = h_1 + (h_2 - h_1)\mathrm{cn}^2(\kappa\,\xi; s),\ \kappa^2 = \frac{3}{4}\frac{(h_2 - h_0)}{h_0h_1h_2},\ s^2 = \frac{h_2 - h_1}{h_2 - h_0},\ \xi = x - Dt. \tag{17}$$

Here the Jacobi elliptic function $cn(u;s)$ is defined as :

$$\mathrm{cn}(u;s) = \cos(\varphi(u,s)),$$

where $\varphi(u,s)$ is obtained implicitly from the relation

$$\int_0^{\varphi} \frac{d\theta}{\sqrt{1-s^2\sin^2(\theta)}} = u.$$

The wave length is given by :

$$\lambda = 2\int_{h_1}^{h_2} \frac{dh}{\sqrt{F(h)}}.$$

The solitary waves correspond to $h_0 = h_1 < h_2$. The solitary waves can be obtained as the limit of periodic waves, when the wave period (wave length) goes to infinity. In the case of solitary waves having the state $h = h_1$ at infinity, the solution is

$$h(\xi) = h_1 + (h_2 - h_1)\mathrm{sech}^2\left(\frac{1}{2}\sqrt{\frac{3(h_2-h_1)}{h_2 h_1^2}}\xi\right),\ \xi = x - Dt,\ D^2 = gh_2.$$

The averaged over the wave length value of any function $f(h)$ is given in the form :

$$\overline{f(h)} = \frac{1}{\lambda}\int_0^{\lambda} f(h(\xi))d\xi = \frac{2}{\lambda}\int_{h_1}^{h_2}\frac{f(h)dh}{\sqrt{F(h)}} = \frac{\int_{h_1}^{h_2}\frac{f(h)dh}{\sqrt{F(h)}}}{\int_{h_1}^{h_2}\frac{dh}{\sqrt{F(h)}}} = \frac{\int_{h_1}^{h_2}\frac{f(h)dh}{\sqrt{P(h)}}}{\int_{h_1}^{h_2}\frac{dh}{\sqrt{P(h)}}}. \tag{18}$$

4 'Thermodynamics' of periodic solutions

This is a classical result which can be found, for example, in [2]. Consider the Lagrangian for the mechanical system with one degree of freedom for unknown v as a function of t:

$$L = \frac{1}{2}\left(\frac{dv}{dt}\right)^2 - W(v, V_1, V_2, ..., V_n). \tag{19}$$

Here W is the potential energy depending on parameters $V_1, V_2, ..., V_n$. The Euler - Lagrange equations for (19) admit the energy integral

$$\frac{1}{2}\left(\frac{dv}{dt}\right)^2 + W(v, V_1, V_2, ..., V_n) = E, \tag{20}$$

where E is the total energy. Let us suppose that (20) admits a periodic solution in a domain of the parameters $V_1, V_2, ..., V_n, E$. Then the period is given by

$$L = \sqrt{2}\int_{v_1}^{v_2}\frac{dv}{\sqrt{E-W}},$$

where v_1, v_2 are simple roots of $E-W=0$ and $E-W>0$ on (v_1,v_2). Let us define the 'temperature' as the average kinetic energy

$$\overline{\frac{1}{2}\left(\frac{dv}{dt}\right)^2}=\frac{\int_0^L \frac{1}{2}\left(\frac{dv}{dt}\right)^2 ds}{L}=\frac{\int_{v_1}^{v_2}\sqrt{E-W}dv}{\int_{v_1}^{v_2}\frac{dv}{\sqrt{E-W}}},$$

and the 'entropy' of the system as

$$S=2\ln\left(\int_{v_1}^{v_2}\sqrt{E-W}dv\right).$$

Then we get the analog of Gibbs identity:

$$\overline{\frac{1}{2}\left(\frac{dv}{dt}\right)^2}dS=dE+\sum_{i=1}^{n}A_i dV_i, \tag{21}$$

where

$$A_i=\overline{-W_{V_i}}=\frac{\int_{u_1}^{u_2}\frac{-W_{V_i}}{\sqrt{E-W}}du}{\int_{u_1}^{u_2}\frac{du}{\sqrt{E-W}}}.$$

In the following, we obtain a system of equations (Whitham's modulation equations [52]) for the parameters representing the averaged quantities describing highly oscillating solutions to dispersive equations. An analogous to (21) 'thermodynamic' relation between averaged quantities will also be derived for the modulation equations.

5 Modulation equations

We resume here some basic results obtained in [11] in the case where $\tilde{e}=\tilde{e}(\tau,\tau_t)$ (inertia type regularization) by averaging conservation laws (6), (8), (9) for the mass, momentum, energy and Bernoulli equations written in mass Lagrangian coordinates. The case where $\tilde{e}=\tilde{e}\,(\tau,\tau_q)$ (capillarity type regularization) was considered, for example, in [12].

We are looking for asymptotic solutions of (6)–(7) with potential $\tilde{e}=\tilde{e}\,(\tau,\tau_t)$. Following Whitham's approach [52] we are looking for the solutions of the form :

$$\begin{pmatrix}\tau\\ u\end{pmatrix}=\begin{pmatrix}\tau(T,X,\theta,\mu)\\ u(T,X,\theta,\mu)\end{pmatrix},\quad T=\mu t,\quad X=\mu q,\quad \theta=\frac{\Theta\,(T,X)}{\mu},$$

where μ is a small positive parameter. The function $\Theta(T,X)$ is called 'phase'. We define the local wave number k and the frequency ω by the relations :

$$k=\Theta_X,\quad \omega=-\Theta_T. \tag{22}$$

We will suppose that the solution is 2π-periodic with with respect to the rapid variable θ. The derivative with respect to θ will be denoted with subscript 'θ', 'bar' means the averaging with respect to the period of θ. We need to substitute this ansatz to obtain in zero order a system of ordinary differential equations with respect to θ. One has in zero approximation the following first integrals :

$$D\tau+u=D\overline{\tau}+\overline{u},\quad -Du+p=-D\overline{u}+\overline{p},\quad D=\frac{\omega}{k}. \tag{23}$$

The system (23) admits the following useful consequences:

$$\overline{u^2} - (\overline{u})^2 = D^2(\overline{\tau^2} - (\overline{\tau})^2), \tag{24}$$

$$\overline{u\tau} - \overline{u}\,\overline{\tau} = -D(\overline{\tau^2} - (\overline{\tau})^2), \tag{25}$$

$$\overline{pu} - \overline{p}\,\overline{u} = D^3(\overline{\tau^2} - (\overline{\tau})^2), \tag{26}$$

$$\overline{p\tau} - \overline{p}\,\overline{\tau} = -D^2(\overline{\tau^2} - (\overline{\tau})^2). \tag{27}$$

In zero approximation, one has :

$$\tilde{e}(\tau, \tau_t) \approx \tilde{e}(\tau, \eta), \quad \eta = -\omega\tau_\theta, \quad p = -\left(\tilde{e}_\tau + \omega\,(\tilde{e}_\eta)_\theta\right). \tag{28}$$

The system (23) also admits the first integral in the form :

$$-D\left(\tilde{e} - \eta\tilde{e}_\eta + \frac{u^2}{2}\right) + pu = -D\left(\overline{\tilde{e} - \eta\tilde{e}_\eta + \frac{u^2}{2}}\right) + \overline{pu}. \tag{29}$$

The integral (29) allows us to obtain the non-linear dispersion relation coming from the fact that the solution is 2π-periodic. In the first order, after the averaging with respect to the rapid variable θ, one obtains the following systems of five compatible conservation laws :

$$\overline{\tau}_T - \overline{u}_X = 0,$$

$$\overline{u}_T + \overline{p}_X = 0,$$

$$\left(\overline{\frac{u^2}{2} + \varepsilon}\right)_T + (\overline{pu})_X = 0, \quad \varepsilon = \tilde{e} - \eta\tilde{e}_\eta,$$

$$\left(\overline{\tau u - k\tau_\theta \frac{\partial \tilde{e}}{\partial \eta}}\right)_T - \left(\overline{\frac{u^2}{2} - \tau p - \tilde{e}}\right)_X = 0,$$

$$k_T + \omega_X = 0.$$

The last equation is just the compatibility condition coming from the definition of (22). It can be also written in the form

$$k_T + (Dk)_X = 0, \quad D = \frac{\omega}{k}.$$

Introducing

$$\Delta = \overline{u\tau} - \overline{u}\,\overline{\tau},\ \overline{\varepsilon} = \overline{\tilde{e} - \eta\tilde{e}_\eta},\ E = \overline{\varepsilon} + \frac{\overline{u^2} - \overline{u}^2}{2},\ \sigma = \overline{\tau_\theta \tilde{e}_\eta},$$

one can obtain a kind of 'Gibbs identity' relating the unknowns (see [11], [12] for proof) :

$$dE + \overline{p}\,d\overline{\tau} + Dd\Delta = \omega d\sigma.$$

It can also be written in the form :

$$d\overline{\varepsilon} + \overline{p}\,d\overline{\tau} - \frac{D^2}{2}d\delta = \omega d\sigma, \quad \delta = \overline{\tau^2} - (\overline{\tau})^2. \tag{30}$$

The Gibbs identity is equivalent to the algebraic 'non-linear dispersion relation' coming from (29) when we are looking for 2π-periodic solution. The mass and momentum equations allow us to obtain a simpler form of (29) :

$$\tilde{e} - \eta\tilde{e}_\eta - \overline{\varepsilon} - \overline{p}\,(\overline{\tau} - \tau) - \frac{D^2}{2}\,(\overline{\tau} - \tau)^2 + \frac{D^2}{2}\delta = 0. \tag{31}$$

In particular, in the case of SGN system the equation (31) has the form :

$$\frac{\omega^2}{6}h_\theta^2 + \frac{gh}{2} - \overline{\varepsilon} - \overline{p}\,(\overline{\tau} - \tau) - \frac{D^2}{2}\,(\overline{\tau} - \tau)^2 + \frac{D^2}{2}\delta = 0, \quad \tau = 1/h. \tag{32}$$

In particular, one can easily see that the equation (15) for travelling waves in the Eulerian coordinates and the equation (32) in the mass Lagrangian coordinates are equivalent, if one takes into account the relation : $\dfrac{\partial h}{\partial x} = h\dfrac{\partial h}{\partial q}$. Thus the averaging procedure introduced here is equivalent to that in Section 3.

Using expressions for correlations (24)–(27), the modulation equations will take the following form :

$$\overline{\tau}_T - \overline{u}_X = 0,$$

$$\overline{u}_T + \overline{p}_X = 0,$$

$$\left(\overline{\varepsilon} + \frac{\overline{u}^2}{2} + \frac{D^2}{2}\left(\overline{\tau^2} - \overline{\tau}^2\right)\right)_T + \left(\overline{p}\,\overline{u} + D^3\left(\overline{\tau^2} - \overline{\tau}^2\right)\right)_X = 0,$$

$$\left(\overline{\tau}\,\overline{u} - D\left(\overline{\tau^2} - \overline{\tau}^2\right) - k\sigma\right)_T - \left(\frac{\overline{u}^2}{2} + \frac{D^2}{2}\left(\overline{\tau^2} - \overline{\tau}^2\right) - \overline{\tau}\,\overline{p} + D^2\left(\overline{\tau^2} - \overline{\tau}^2\right) - \overline{\varepsilon} + \omega\sigma\right)_X = 0,$$

$$k_T + \omega_X = 0.$$

These five conservation laws for only four unknown variables k, D, $\overline{\tau}$, $\overline{u}$: have a clear physical interpretation. Moreover, they are compatible : the averaged Bernoulli law is a consequence of the mass, momentum, energy and phase conservation laws. This can be proved by direct calculations. Using the (5) or (30) one can derive the sixth conservation law for σ ('entropy' conservation law):

$$\left(\sigma + \frac{D\delta}{k}\right)_T + \left(\frac{D^2\delta}{k}\right)_X = 0. \tag{33}$$

For proof, one can use the energy conservation law in the form :

$$\left(\overline{\varepsilon} + \frac{\overline{u}^2}{2} + \frac{D^2}{2}\delta\right)_T + \left(\overline{p}\,\overline{u} + D^3\delta\right)_X = 0.$$

Developing it and using Gibbs relation (30) one obtains :

$$-\overline{p}\,\overline{\tau}_T + \frac{D^2}{2}\delta_T + \omega\sigma_T + \overline{u}\,\overline{u}_T + \frac{D^2}{2}\delta_T + DD_T\delta + \overline{p}_X\overline{u} + \overline{p}\,\overline{u}_X + D(D^2\delta)_X + D^2D_X\delta = 0.$$

Using the mass and momentum equations, one gets :

$$D^2\delta_T + \omega\sigma_T + DD_T\delta + D(D^2\delta)_X + D^2\delta D_X = 0.$$

Or, dividing by D :

$$(D\delta)_T + k\sigma_T + (D^2\delta)_X + D\delta D_X = 0.$$

Dividing by k, one obtains after some algebra the conservation law (33). Finally, the Whitham system admits the conservation laws corresponding to the mass, momentum, energy, Bernoulli, phase and 'entropy' σ.

6 Shocks in Whitham's system

Shocks in Whitham's system are in somewhat 'forbidden', because they would correspond to the appearance of waves having different phases, while we looked only for one-phase solutions [52]. However, one can think about shocks separating solutions having different but single phases. In this case a natural question is the choice of the corresponding Rankine-Hugoniot relations because for four unknowns we have at least six 'reasonable' conservation laws. Let us show that the case where the velocity of the shock is equal to the phase velocity is compatible with five conservation laws from six. The conservation law (33) for the 'entropy' σ will correspond to an inequality.

Consider the Rankine–Hugoniot relations for this system :

$$[V\overline{\tau} + \overline{u}] = 0,$$

$$[-V\overline{u} + \overline{p}] = 0,$$

$$\left[-V\left(\overline{\varepsilon} + \frac{\overline{u}^2}{2} + \frac{D^2}{2}\left(\overline{\tau^2} - \overline{\tau}^2\right)\right) + \overline{p}\,\overline{u} + D^3\left(\overline{\tau^2} - \overline{\tau}^2\right)\right] = 0,$$

$$\left[-V\left(\overline{\tau}\,\overline{u} - D\left(\overline{\tau^2} - \overline{\tau}^2\right) - k\sigma\right) - \left(\frac{\overline{u}^2}{2} + \frac{D^2}{2}\left(\overline{\tau^2} - \overline{\tau}^2\right) - \overline{\tau}\,\overline{p} + D^2\left(\overline{\tau^2} - \overline{\tau}^2\right) - \overline{\varepsilon} + \omega\sigma\right)\right] = 0,$$

$$[-Vk + \omega] = 0.$$

Here V is the shock velocity, and, as usually, $[f] = f^+ - f^-$ for any function f having the limit values f^+ and f^- on the right and on the left, respectively.

Consider a special case where the shock velocity is equal to the phase velocity : $V = D^- = D^+$, $D^\pm = \frac{\omega^\pm}{k^\pm}$:

$$-Vk^- + \omega^- = -Vk^+ + \omega^+.$$

Then the phase conservation law is obviously satisfied, and the shock can relate the states having different values of the wave numbers. Also, it is not necessary that both left and right states correspond to a nontrivial periodic solution. One of them could be degenerate : for example, if $k^+ = 0$, $\omega^+ = 0$, one should has $-Vk^- + \omega^- = 0$. In the last case, one can speak about the discontinuity relating 'hot' state (periodic state with $k \neq 0$, $\omega \neq 0$) and 'cold' state ($k = 0$, $\omega = 0$).

Let us first show that the shock relations coming from the averaged energy equation and the averaged Bernoulli law are compatible in the presence of such special shocks. The Bernoulli law can be written in the form (we used here the mass and momentum conservation laws):

$$\left[-V\left(\overline{\varepsilon} + \frac{\overline{u}^2}{2}\right) + \overline{p}\,\overline{u} + \frac{D^3}{2}\left(\overline{\tau^2} - \overline{\tau}^2\right)\right] = 0,$$

$$\left[V\overline{\tau}\,\overline{u} + \frac{\overline{u}^2}{2} + \frac{D^2}{2}\left(\overline{\tau^2} - \overline{\tau}^2\right) - \overline{\tau}\,\overline{p} - \overline{\varepsilon}\right] = 0.$$

Multiplying the second equation by V, subtracting the equations and taking again into account that $V = D$, we obtain :

$$[(\overline{u} + V\overline{\tau})\,(\overline{p} - V\overline{u})] = 0.$$

The last identity is a direct consequence of the mass and momentum equations. Thus, the Bernoulli and energy laws are compatible for shocks having property $V = D$ (the shock velocity coincides with the phase velocity of travelling waves). Moreover, the entropy inequality coming from (33) will take now a very simple form reminiscent of a classical entropy inequality for the Euler equations of compressible fluids :

$$-V\,[\sigma] \geq 0. \tag{34}$$

The only questions appear here are : do these solutions exist? are these solutions stable? We will study this question for the SGN system numerically in the next Section.

7 Generalized Riemann problem

The numerical study will be performed in the Eulerian coordinates, since it allows us to better interpret the results obtained. Thus, the averaging will be understood in the sense of the definition (18). We denote by $h_s(\xi)$, $u_s(\xi)$, $\xi = x - Dt$ the travelling wave solution to the SGN equations. The aim of this section is to solve numerically a special Riemann problem with a periodic stationary solution on the left, and another one on the right. To put in evidence the importance of dispersion, consider the Riemann problem where initially the non-trivial periodic solution is in contact with a constant solution having the same averaged data. To have a possibility to properly invert the elliptic operator for the SGN equations (cf. [32]), we will bound the periodic solution by the same averaged constant values:

$$\begin{pmatrix} h(0,x) \\ u(0,x) \end{pmatrix} = \begin{cases} \begin{pmatrix} h_R = \overline{h_s} \\ u_R = 0 \end{pmatrix}, & \text{if } x > L, \\ \begin{pmatrix} h_s(x) \\ u_s(x) \end{pmatrix}, & \text{if } -L < x < L, \\ \begin{pmatrix} h_L = \overline{h_s} \\ u_L = 0 \end{pmatrix}, & \text{if } x < -L. \end{cases} \tag{35}$$

Here $(h_s(x),\, u_s(x))$ is a periodic solution to the SGN equations, having the average values $(\overline{h}_s(x),\, \overline{u}_s(x) = 0)$. In the pure hyperbolic case such a problem has only a trivial constant solution, while in the dispersive case we will see a striking difference in the solution behavior.

The periodic solution depends on four constants. The first three constants are h_0, h_1, h_2 mentioned above. The forth one is the wave velocity D. They determine completely the fluid depth $h_s(x)$. Finally, to calculate the velocity $u_s(x)$, we need to use the mass conservation law :

$$h_s(u_s - D) = m.$$

For $m = -\sqrt{gh_0h_1h_2}$ given (for definiteness, we choose the sigh 'minus' corresponding to the periodic waves moving to the right), we have :

$$(u_s - D) = mh_s^{-1}.$$

It implies

$$D = \overline{u_s} - m\overline{h_s^{-1}}.$$

Obviously,

$$\text{sign}(u_s - D) = \text{sign}(\overline{u}_s - D).$$

In particular, we will choose the following values of D :

$$D = -m\left(\overline{h_s^{-1}}\right). \tag{36}$$

In this case we obviously have $\overline{u_s} = 0$. Finally, to have a stationary periodic wave in the middle (this is useful for numerics), we use the Galilean invariance of the governing equations to replace $u_{R,L} = 0$ by $-D$.

8 Froude number

For this special generalized Riemann problem (35), the Froude number (the analogue of the Mach number in aerodynamics) is used to characterize the flow as supercritical ($Fr > 1$), or subcritical ($Fr < 1$), or critical ($Fr = 1$). We define the Froude number as :

$$Fr = \frac{D}{\sqrt{g\overline{h_s}}} = \frac{-m\overline{h_s^{-1}}}{\sqrt{g\overline{h_s}}} = \sqrt{h_0h_1h_2}\frac{\overline{h_s^{-1}}}{\sqrt{\overline{h_s}}}.$$

Let us make the change of variables

$$h = h_1 + t(h_2 - h_1), \quad 0 \le t \le 1.$$

Then

$$\begin{aligned} P(h) &= t(1-t)(h_2-h_1)^2(h_1-h_0+t(h_2-h_1)) = t(1-t)(h_2-h_1)^2(h_2-h_0-(1-t)(h_2-h_1)) \\ &= (h_2-h_0)(h_2-h_1)^2t(1-t)(1-s^2(1-t)), \end{aligned}$$

with

$$s^2 = \frac{h_2-h_1}{h_2-h_0}. \tag{37}$$

The Froude number can be expressed as :

$$\begin{aligned} Fr &= \sqrt{h_0h_1h_2}\frac{\overline{h_s^{-1}}}{\sqrt{\overline{h_s}}} \\ &= \sqrt{h_0h_1h_2}\frac{\int_0^1 \frac{dt}{(h_1+t(h_2-h_1))\sqrt{t(1-t)(1-s^2(1-t))}}}{\sqrt{\int_0^1 \frac{(h_1+t(h_2-h_1))dt}{\sqrt{t(1-t)(1-s^2(1-t))}}}\sqrt{\int_0^1 \frac{dt}{\sqrt{t(1-t)(1-s^2(1-t))}}}} \\ &= \sqrt{\frac{h_0h_2}{h_1^2}}\frac{\int_0^1 \frac{dt}{(1+c^2t)\sqrt{t(1-t)(1-s^2(1-t))}}}{\sqrt{\int_0^1 \frac{(1+c^2t)dt}{\sqrt{t(1-t)(1-s^2(1-t))}}}\sqrt{\int_0^1 \frac{dt}{\sqrt{t(1-t)(1-s^2(1-t))}}}}, \end{aligned}$$

where

$$c^2 = \frac{h_2}{h_1} - 1. \tag{38}$$

Changing the independent variable t by θ :

$$t = \cos^2(\theta)$$

we finally obtain :

$$Fr = \sqrt{\frac{h_0 h_2}{h_1^2}} \frac{\int_0^{\pi/2} \frac{d\theta}{(1+c^2\cos^2(\theta))\sqrt{1-s^2\sin^2(\theta)}}}{\sqrt{\int_0^{\pi/2} \frac{(1+c^2\cos^2(\theta))d\theta}{\sqrt{1-s^2\sin^2(\theta)}}} \sqrt{\int_0^{\pi/2} \frac{d\theta}{\sqrt{1-s^2\sin^2(\theta)}}}}, \tag{39}$$

where s^2 and c^2 are defined by (37) and (38), respectively.

It appears that the criticality condition $Fr = 1$ given by (39) plays an important role in the analysis of the generalized Riemann problem (35). The expression $Fr = 1$ can obviously be rewritten as a function of dimensionless parameters $(H_1, H_2) = (h_1/h_0, h_2/h_0)$. This curve is shown in Figure 1.

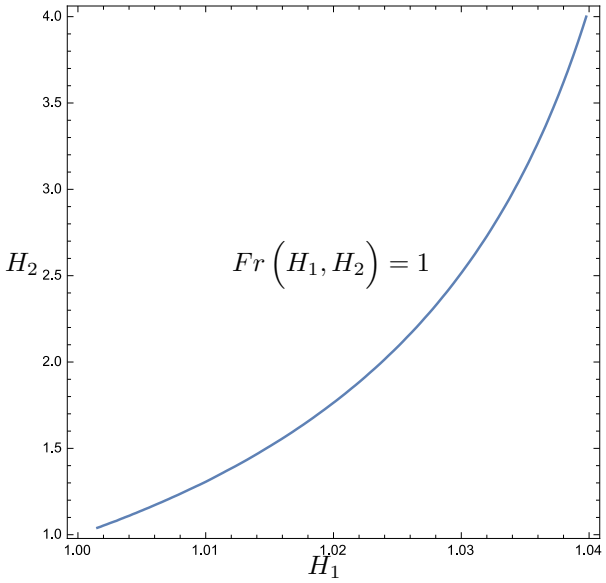

Figure 1: The continuous line at the plane $(H_1 = h_1/h_0,\ H_2 = h_2/h_0)$ is the curve defined implicitly by the relation $Fr = 1$ (see the expression (39) of the Froude number), where c^2 and s^2 are defined by (38) and (37), respectively.

9 'Cold' and 'hot' conjugate states

As we have seen before, the periodic solution depends on four constants, which can be fixed by the mass, momentum and energy first integrals, and a forth constant which can be taken as the wave velocity D. We ask the following question : is it possible to somehow connect the periodic solution to SGN equations with a constant state in a weak sense. This is very different from the classical

question about dispersive shocks where two constant states are connected via dispersive shock [19], [7], [8].

We will show that the 'cold' and 'hot' states (constant and periodic states, respectively) can be connected to each other, if they are shock solutions to Whitham's equations (modulation equations) derived in Section 5. As it was already discussed, these shocks are quite specific : the shock velocity coincides with the velocity of periodic travelling waves. If such a solution to Whitham's system exists, it would correspond also to a discontinuous solution to the full dispersive SGN system. This fact would be very unexpected, because usually the dispersion leads to the smoothing of the initial discontinuity. However, some types of dispersion cannot prevent from the appearance of discontinuous solutions. This is, for example, a discontinuous solution to BBM equation constructed in [9], which is at the same time a solution to the Hopf equation. The Riemann problem (35) for SGN equation in the case where the periodic initial data in the middle is stationary ($D = 0$) is :

$$\begin{pmatrix} h(0,x) \\ u(0,x) \end{pmatrix} = \begin{cases} \begin{pmatrix} h_R = \overline{h_s} \\ u_R = m\left(\overline{h_s^{-1}}\right) \end{pmatrix}, & \text{if } x > L, \\ \begin{pmatrix} h_s(x) \\ u_s(x) \end{pmatrix}, & \text{if } -L < x < L, \\ \begin{pmatrix} h_L = \overline{h_s} \\ u_L = m\left(\overline{h_s^{-1}}\right) \end{pmatrix}, & \text{if } x < -L, \end{cases} \tag{40}$$

Our 'experimental' (numerical) observation is as follows. If one takes the values of h_0, h_1 and h_2 at the vicinity of the critical curve $Fr(H_1, H_2) = 1$, a stationary shock connecting the initial stationary periodic wave train ('hot' state) and a new dynamically formed constant ('cold') state appears in the solution of the generalized Riemann problem (40). This stationary shock is a weak solution to the SGN equations : it is a shock solution for the corresponding Whitham equations. Through such a shock the Rankine-Hugoniot relations to Whitham's system are satisfied : the mass, momentum, energy, Bernoulli equation and phase equation. The 'entropy' equation will play exactly the same role as in the Euler equation of compressible fluids : it will just indicate the entropy increase behind the shock (a 'hot' state will appear). Such a shock transforms a constant 'cold' state (denoted by 'star') into an oscillating wave train ('hot' state).

The conjugate 'hot' and 'cold' states verify the Rankine–Hugoniot relations written here in the Eulerian coordinates :

$$hu = \overline{hu} = h_\star u_\star = m,$$

$$hu^2 + \frac{gh^2}{2} + \frac{m^2}{3} h \frac{d}{d\xi}\left(\frac{1}{h}\frac{dh}{d\xi}\right) = \overline{hu^2 + \frac{gh^2}{2} + \frac{m^2}{3} h \frac{d}{d\xi}\left(\frac{1}{h}\frac{dh}{d\xi}\right)} = h_\star u_\star^2 + \frac{gh_\star^2}{2} = \frac{m^2}{h_\star} + \frac{gh_\star^2}{2},$$

$$\frac{u^2}{2} + gh + \frac{m^2}{6h^2}\left(\frac{dh}{d\xi}\right)^2 = \overline{\frac{u^2}{2} + gh + \frac{m^2}{6h^2}\left(\frac{dh}{d\xi}\right)^2} = \frac{m^2}{2h_\star^2} + gh_\star.$$

They correspond to the Rankine – Hugoniot relations for Whitham's system. Here 'star' corresponds to the constant 'cold' state. Since

$$h \frac{d}{d\xi}\left(\frac{1}{h}\frac{dh}{d\xi}\right) = \frac{d^2h}{d\xi^2} - \frac{1}{h}\left(\frac{dh}{d\xi}\right)^2,$$

and the average of the derivative of a periodic function vanishes, one obtains the following generalized Rankine-Hugoniot relations :

$$hu = \overline{hu} = h_\star u_\star = m, \tag{41}$$

$$\frac{m^2}{h}+\frac{gh^2}{2}-\frac{m^2}{3h}\left(\frac{dh}{d\xi}\right)^2=\overline{\frac{m^2}{h}+\frac{gh^2}{2}-\frac{m^2}{3h}\left(\frac{dh}{d\xi}\right)^2}=\frac{m^2}{h_\star}+\frac{gh_\star^2}{2}, \tag{42}$$

$$\frac{m^2}{2h^2}+gh+\frac{m^2}{6h^2}\left(\frac{dh}{d\xi}\right)^2=\overline{\frac{m^2}{2h^2}+gh+\frac{m^2}{6h^2}\left(\frac{dh}{d\xi}\right)^2}=\frac{m^2}{2h_\star^2}+gh_\star. \tag{43}$$

Equations (41)–(43) can only be fulfilled for special values of $h_\star$ because one has to satisfy for a given m, the momentum and energy equation for only one variable $h_\star$.

Since $m^2=gh_0h_1h_2$, one can easily see from (41), (42), (43) that the value of $h_\star$ is determined only by h_0, h_1, h_2, and not by the value of constant g (acceleration of gravity). However, the value of $u_\star$ depends on g.

Let us also remark that the SGN equations admit a forth conservation law (12) (Bernoulli law). The generalized Rankine-Hugoniot relation corresponding to (12) would be:

$$Ku+gh-\frac{u^2}{2}-\frac{h^2}{2}\left(\frac{du}{d\xi}\right)^2=\overline{Ku+gh-\frac{u^2}{2}-\frac{h^2}{2}\left(\frac{du}{d\xi}\right)^2}=\frac{u_\star^2}{2}+gh_\star=\frac{m^2}{2h_\star^2}+gh_\star. \tag{44}$$

One needs to finally understand if the integrals (41), (42), (43) and (44) can be satisfied through the shock at some choice of the initial parameters.

We will prove this claim by using a numerical approach. The numerical method is described in Section 11, and we take the same version of the method as performed for the dam-break problem considered in Section 11.3.3 during the simulation. For definiteness, we will choose the dimension parameters determining the periodic stationary wave train as $h_0=1.0962\ m$, $h_1=1.1\ m$, $h_2=1.2\ m$ and $g=10\ m/s^2$. They satisfy the relation $Fr=1$. The corresponding shock velocity D determined by (36) is $3.36413\ m/s$. One can easily find by using, for example, Wolfram Mathematica, that for these parameters $h_\star=1.09808\ m$ and $u_\star=-3.46416\ m/s$. So, formally, the state 'star' can be adjacent to a periodic solution through a stationary shock.

In Figure 2, the initial data for the Riemann problem (40) are shown. The initial wave height and velocity are discontinuous on the left and on the right. A sketch of the first single stationary wave on the left is shown in Figure 3. The numerical solution of the Riemann problem (40) to SGN equations is shown in Figure 4 at time instant $1000\ s$. A new constant 'cold' state is formed on the left, between a left going rarefaction wave and the initial periodic wave train. The theoretical values of this 'star' state coincide with the corresponding numerical values. A magnified view of this new 'star' state is shown in Figure 5. The space distribution of wave lengths shows that the left part of the periodic wave train is not at all perturbed. Thus, a stationary shock relating the 'star' solution and periodic wave train verifying the Rankine–Hugoniot relations for the corresponding Whitham equations is formed. On the right part of the wave train one can see the formation of a right facing dispersive shock (Figure 4).

Finally, we will take the initial data shown in Figure 6. The only difference between the initial data shown in Figure 2 and those in Figure 6 is that 'star' state is put on the left : $h_\star=1.09808\ m$ and $u_\star=-3.46416\ m/s$. The value of $h_\star$ is smaller than that of h_1 (see Figure 7). We will now prove that if one initially takes state 'star' (determined analytically from (41), (42), (43) and (44)) on the left, then it will be not perturbed until a left going wave arrives from the right. Thus, this will be a numerical proof of stability of weak solution to SGN model. This fact can be observed from Figures 8 (computation are shown at time instant $400\ s$) and Figure 9 (at time instant $1000\ s$.)

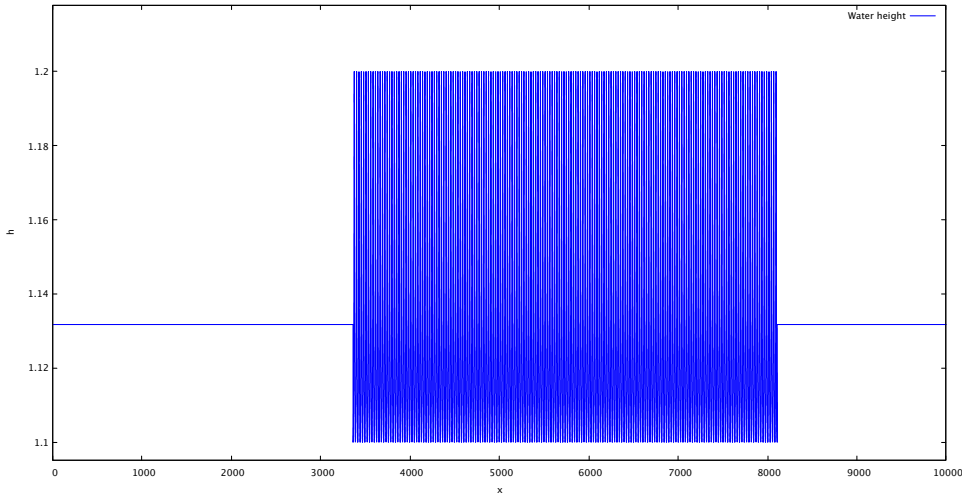

Figure 2: The initial condition for the water depth h of the generalized Riemann problem (40) in the case where the water heights for the single travelling wave solution are $h_0 = 1.0962\ m$, $h_1 = 1.1\ m$, and $h_2 = 1.2\ m$ corresponding to a periodic wave of length $\lambda = 26.3767\ m$. The wave packet in the middle is made up of 180 single stationary wave solutions, and constant state on the left and right is equal to the average value of the over the period : $\overline{h_s} = 1.13173\ m$.

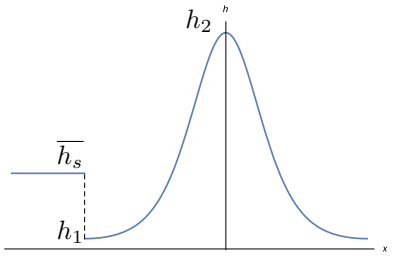

Figure 3: The initial wave hight and velocity are discontinuous on the left and on the right. A sketch of the first single stationary wave on the left is shown which is connected to the constant state $\overline{h}_s$ whose value corresponds to the average one over the wave period.

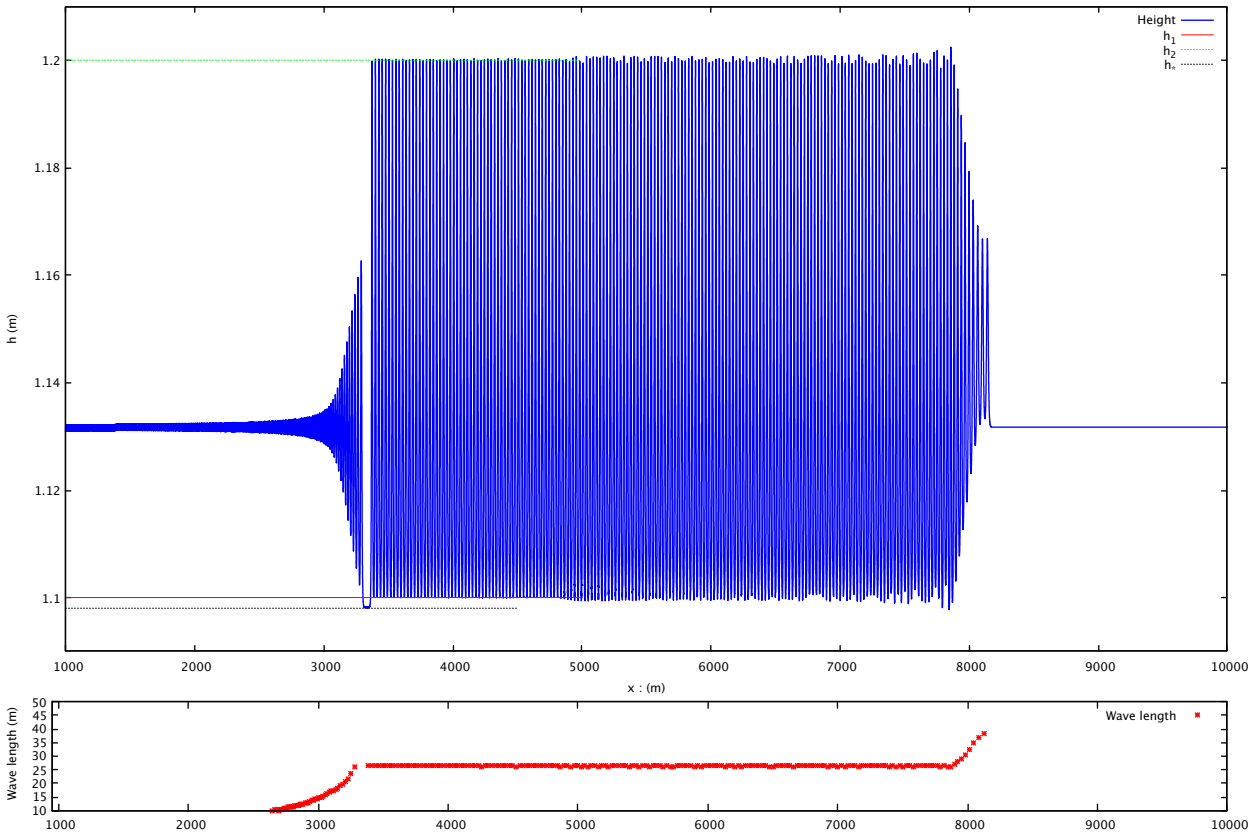

Figure 4: Numerical solution of the generalized Riemann problem at time $t = 1000\ s$; the initial condition is the one shown in Fig. 2.

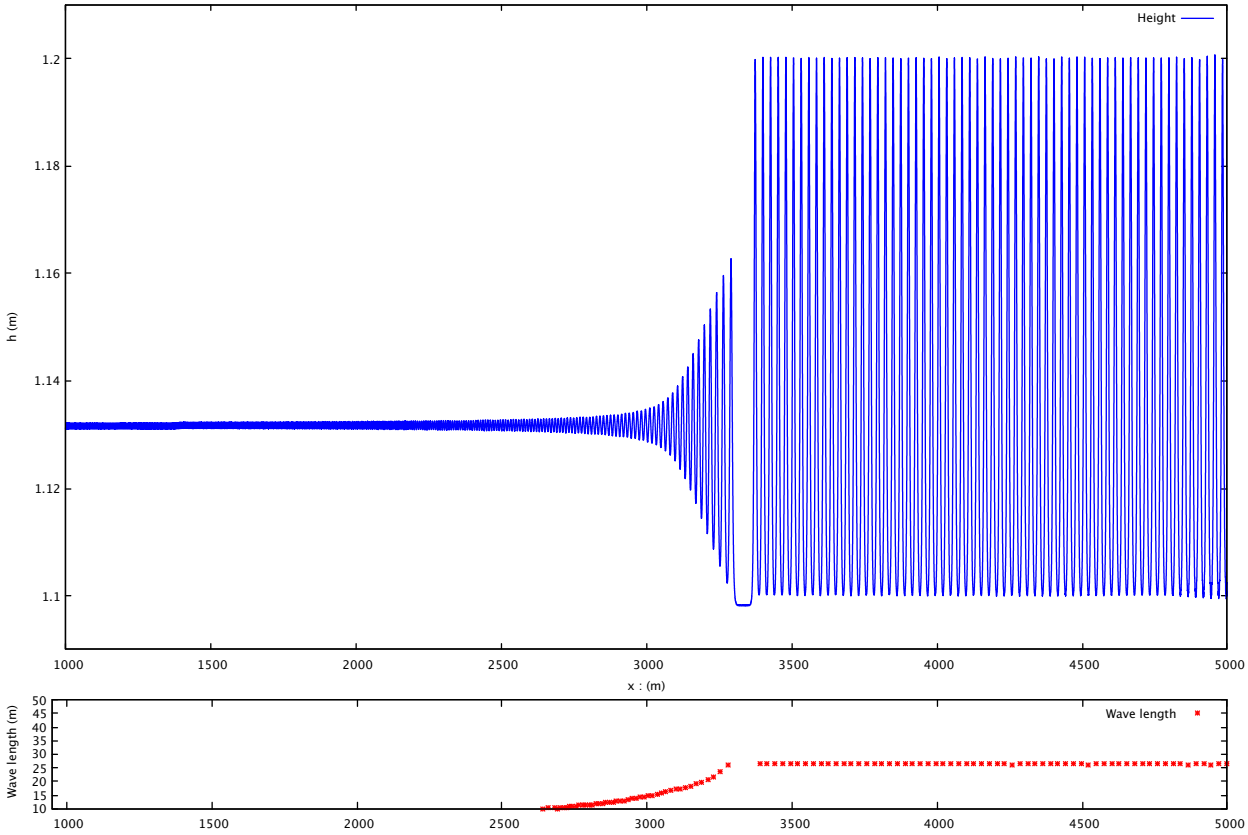

Figure 5: A magnified view of the numerical solution of the generalized Riemann problem on the left boundary at $t = 1000\ s$. The space distribution of wavelengths (the distance between nearby local maxima of waves) is shown at the bottom by red stars. The appearance of a new constant state related by a shock with a periodic wave train is clearly visible.

Figure 10 shows the flow picture at time instant 6000 s. Small perturbations have already passed through the stationary shock on the left. The initial periodic wave train is also a little bit perturbed, and fills a smaller region compared to its initial one. Remarkable, it is related by a long transition zone with a new right 'periodic state'. Indeed, one can see at the bottom of Figure 10 the length distribution transition : from one plateau to another one. The new periodic state on the right has a larger length. It is separated from the right constant state over a very shot distance. We call this new periodic state 'solitary' wave train. Indeed, compared to the initial periodic wave train having the average depth equal to the constant depth on the right, this wave train has the average depth which is always greater than the constant depth on the right. Locally, each wave can be considered as a soliton : these waves form thus a solitary wave train. So, the transition from a 'hot' state to a 'cold' one happens, but this new cold state is formed by solitons. The averaged kinetic energy related to the high amplitude oscillations is decreasing in space and transforms to the average potential energy (see Figure 11). Such a transition corresponds to the rarefaction wave of the Whitham system.

The full structure of the solution of the generalized Riemann problem to SGN equations is still not well understood. However, as we show in Section 10, the phenomenon of formation of an adjacent to a periodic solution constant state is quite generic, and it happens even in the case of linear dispersion. A further study is needed for the variety of unresolved issues and questions.

10 Comparaison between SGN and Boussinesq-type models

There exists a large number of Boussinesq-type approximations to SGN equations. The simplest one is to replace the nonlinear dispersion term in (10) by a linear one :

$$h_t + (hu) = 0, \quad (hu)_t + (hu^2 + p) = 0, \quad p = \frac{gh^2}{2} + \frac{\bar{h}_0^2}{3} h_{tt}. \tag{45}$$

Here $\bar{h}_0$ is a constant. We wonder if the shocks can also be formed in this case. The travelling wave solutions to (45) depending on $\xi = x - Dt$ satisfy the equations :

$$h(u - D) = m = const, \ \frac{m^2}{h} + \frac{g}{2} h^2 + \frac{D^2 \bar{h}_0^2}{3} h'' = i = const. \tag{46}$$

Here m and i are integration constants. Multiplying the equation by h' and integrating it once, one obtains:

$$\frac{D^2 \bar{h}_0^2}{6} (h')^2 = ih - \frac{gh^3}{6} - m^2 \ln\left(\frac{h}{H}\right). \tag{47}$$

Here H is a new positive integration constant. The condition of existence of three real positive roots $0 < h_0 < h_1 < h_2$ of the right-hand side of (47) is that the following equation has two positive roots :

$$\frac{m^2}{h} + \frac{g}{2} h^2 = i. \tag{48}$$

In this case the periodic solution oscillates between h_1 and h_2. If one takes $i = 19.22372308$, $m^2 = 14.4889747$, $H = 0.297886$, one gets the same roots as in the case of periodic solutions to SGN equations : $h_0 = 1.0962$, $h_1 = 1.1$ and $h_2 = 1.2$. All the numerical values are expressed in the

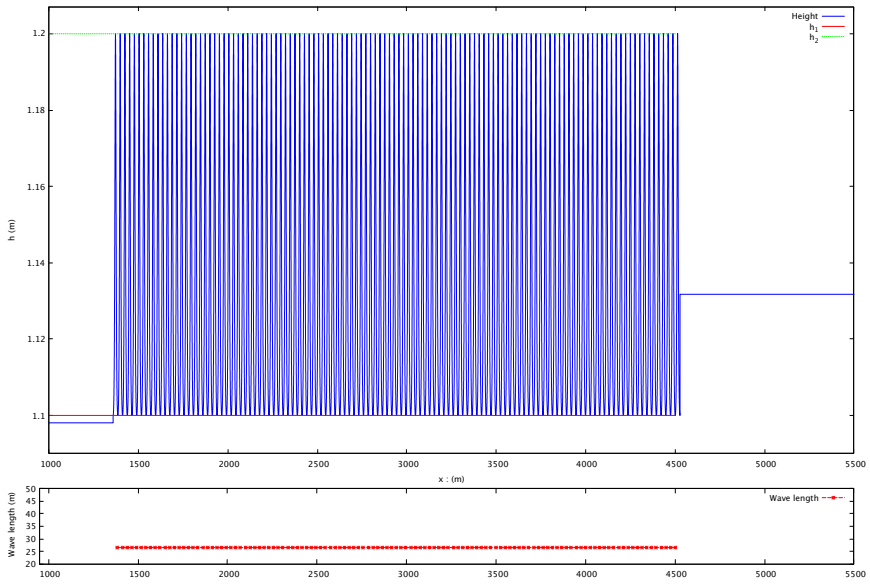

Figure 6: The initial condition for the generalized Riemann problem with the 'star' state on the left portion of the domain; the remaining portions of the domain take the same data as in Fig. 2. At the bottom, a space distribution of the wavelengths (the distance between nearby local maxima of waves) is shown by red stars. Initially, it is uniform.

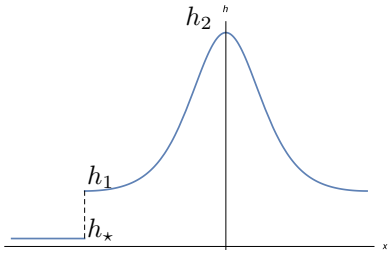

Figure 7: The initial wave hight and velocity are discontinuous on the left and on the right. A sketch of the first single wave on the left is shown which is connected to the constant state $h_\star$ found earlier.

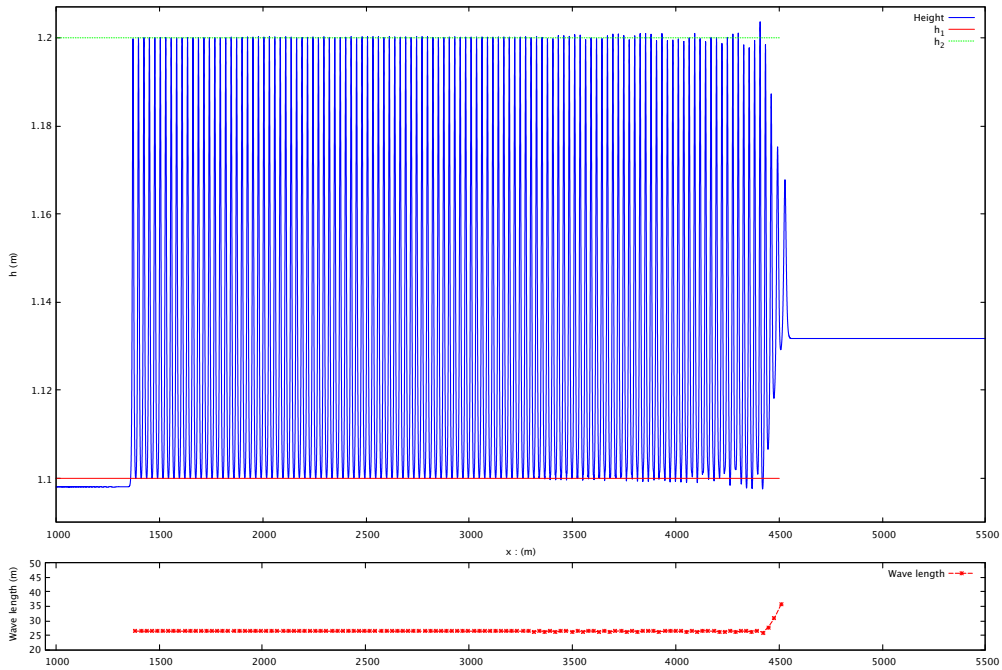

Figure 8: Numerical solution of the generalized Riemann problem at time $t = 400\ s$; the initial condition is the one shown in Fig. 6.

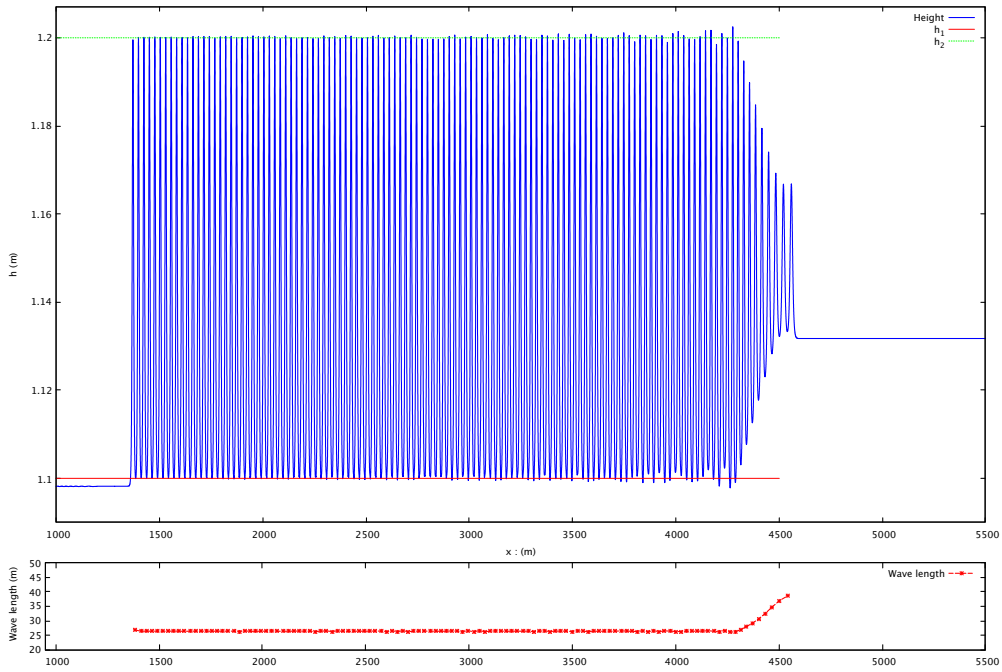

Figure 9: Numerical solution of the generalized Riemann problem at time $t = 1000\ s$; the initial condition is the one shown in Fig. 6.

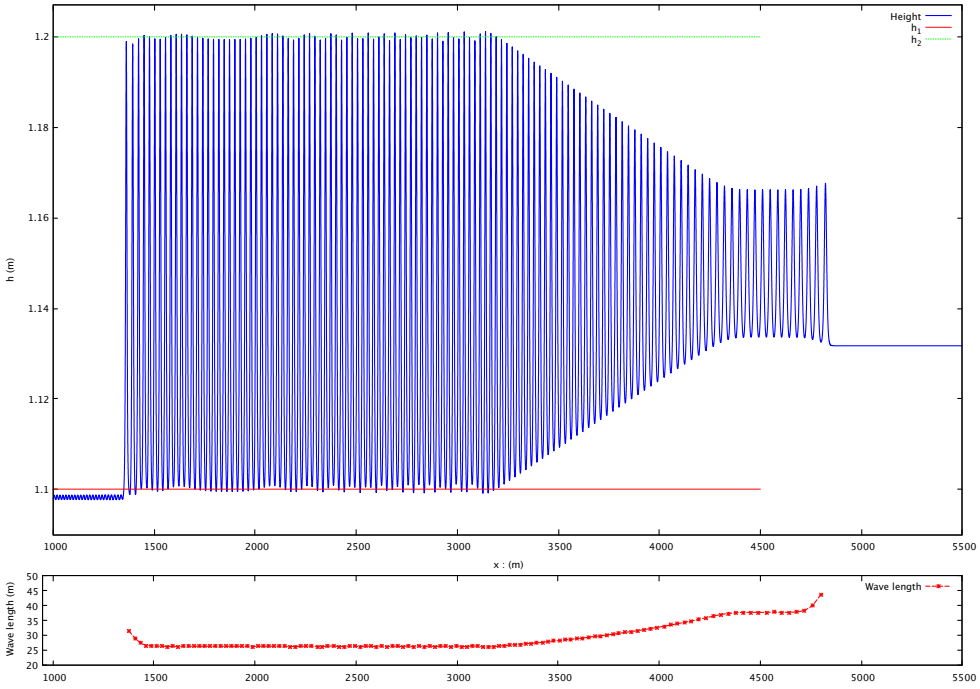

Figure 10: Numerical solution of the generalized Riemann problem at time $t = 6000\ s$; the initial condition is the one shown in Fig. 6. At the bottom, the distribution of waves is shown. Remarkable, a transition from a periodic wave train to a solitary wave train occurs.

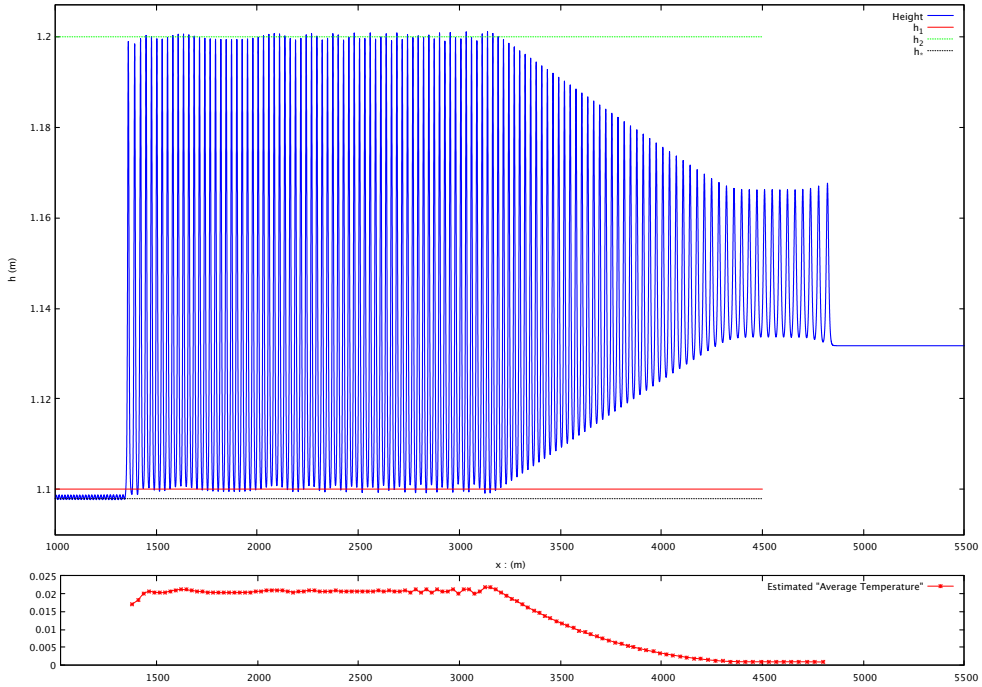

Figure 11: Numerical solution of the generalized Riemann problem at time $t = 6000\ s$; the initial condition is the one shown in Fig. 6. At the bottom, the distribution of the pulsation energy $\frac{1}{\lambda}\int_0^\lambda \left(\frac{Dh}{Dt}\right)^2 dx$ averaged over the period λ is shown (multiplied by 20 for a better visibility). It is decreasing in space, a transition from a 'hot' to a 'cold' state occurs, the local 'average temperature' transforms into potential energy : the right facing periodic wave is rather a 'solitary' wave train.

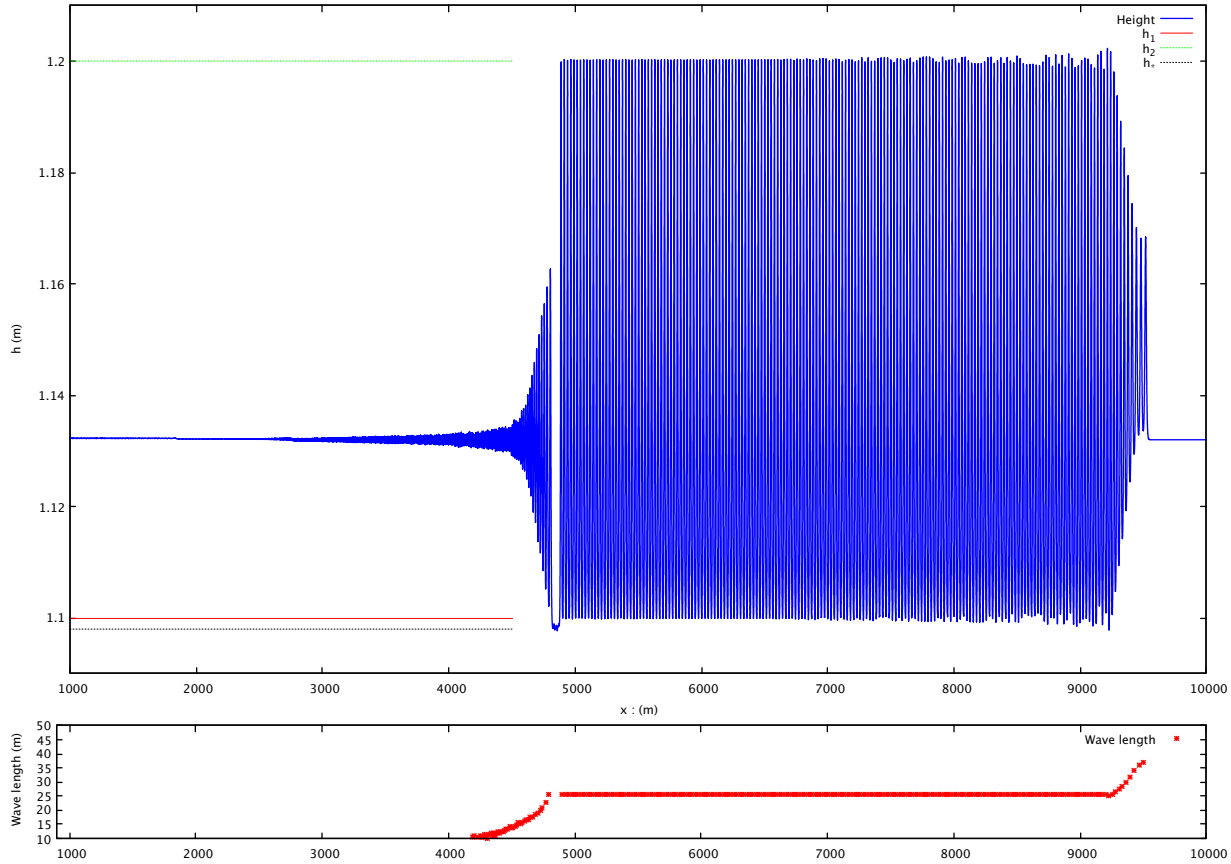

Figure 12: Numerical solution of the generalized Riemann problem at time $t = 1000$ s for Boussinesq system (45) is shown. At the bottom, the distribution of wave lengths is given. A shock solution is formed which is reminiscent of that obtained for SGN equations (see Figure 4).

SI units. One can find then the corresponding wave length :

$$\lambda = \frac{2D\bar{h}_0}{\sqrt{6}} \int_{h_1}^{h_2} \frac{dh}{\sqrt{ih - \frac{gh^3}{6} - m^2 \ln\left(\frac{h}{H}\right)}}. \tag{49}$$

Let us also fix the same velocity D as in the generalized Riemann problem for SGN equations. It gives us the wave length. The main difference between SGN model and Boussinesq model is that the last model is no longer invariant under Galilean transformation. In particular, it implies that the wave length in Boussinesq model will depend also on D. The numerical results are shown in Figures 12 and 13. One can see, as in the case of SGN equations, the formation of a shock wave separating 'cold' and 'hot' states.

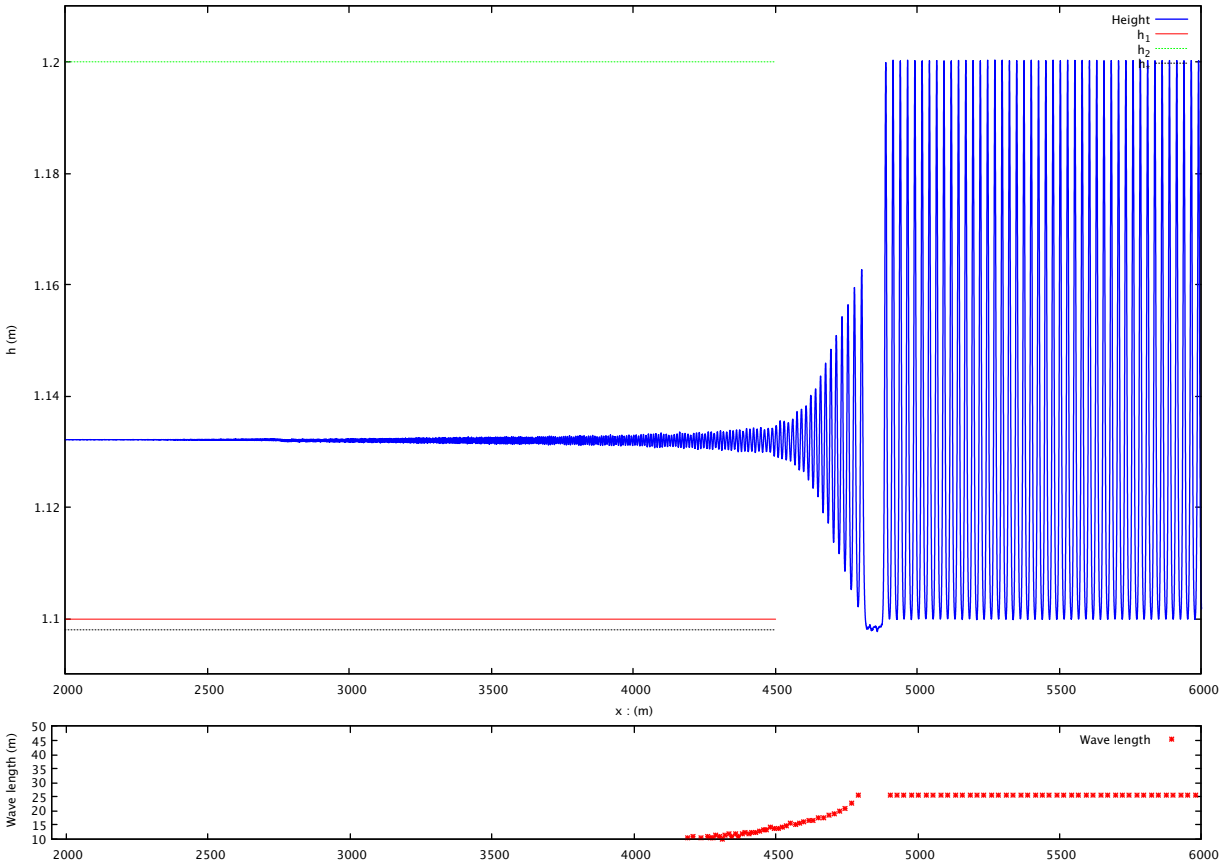

Figure 13: Numerical solution of the generalized Riemann problem at time $t = 1000$ s for Boussinesq system (45) is shown (magnified view).

11 Numerical method

To find approximate solutions to SGN equations, we are interested in a hyperbolic-elliptic splitting approach developed previously in [32]. A modified version of this algorithm will consists of the following two steps:

Hyperbolic step.
We solve the hyperbolic part of system (10) of the form :

$$\boldsymbol{q}_t + \boldsymbol{f}(\boldsymbol{q}, u)_x = \boldsymbol{\psi}(\boldsymbol{q}, u) \tag{50a}$$

with the conservative variable $\boldsymbol{q}$, the flux function $\boldsymbol{f}$, and the source term $\boldsymbol{\psi}$ defined by $\boldsymbol{q} = (h, hK)^T$, $\boldsymbol{f} = \left(hu, hKu + \frac{1}{2}gh^2\right)^T$, and $\boldsymbol{\psi} = \left(0, \left(\frac{2}{3}h^3 \left(u_x\right)^2\right)_x\right)^T$, respectively, over a time step Δt.

Elliptic step.
With the approximate solutions h and K computed from the hyperbolic step, the following Helmholtz equation in u is inverted numerically:

$$u - \frac{1}{3h}\left(h^3 u_x\right)_x = K \tag{50b}$$

with prescribed boundary conditions.

Note that in the hyperbolic step, rather than writing (50a) in a conservation form as in [32] with $\boldsymbol{f} = \left(hu, hKu + \frac{1}{2}gh^2 - \frac{2}{3}h^3 \left(u_x\right)^2\right)^T$ and $\boldsymbol{\psi} = \boldsymbol{0}$, which is ideal to be employed in a conservative first-order method (cf. [28]), but is difficult to be extended to more than first order accurate (see below), it is written in a balance form instead with an aim to have a more robust higher-order hyperbolic solver. We have a standard elliptic problem to be solved in the elliptic step, and so, in principle, any state-of-the-art method can be used for the numerical resolution of this elliptic problem (cf. [29, 45]). Our goal next is to describe each of the steps in more detail.

11.1 Numerical method for hyperbolic step

To compute solutions to SGN equations in the hyperbolic step, we use the semi-discrete finite volume method written in a wave-propagation form (cf. [25, 26]). This method belongs to the class of flux-vector splitting methods for hyperbolic conservation laws [18, 28, 47], and has been applied to compressible multiphase flows (cf. [43]), and in other instances of practical importance. For simplicity, we describe the method on a uniform grid of N cells with fixed mesh spacing Δx. The method is based on a staggered grid formulation in which the value $\boldsymbol{Q}_j(t)$ approximates the cell average of the solutions $\mathbf{q}$ over the grid cell C_j :

$$\boldsymbol{Q}_j(t) \approx \frac{1}{\Delta x}\int_{x_{j-1/2}}^{x_{j+1/2}} \boldsymbol{q}(t, x)\, dx,$$

while $U_j(t) \approx u(t, x_j)$ gives the pointwise approximation of the velocity u at x_j at time t.

The semi-discrete version of the wave-propagation method is a method-of-lines discretization of (50a) that can be written as a system of ordinary differential equations (ODEs) in the form :

$$\frac{d\boldsymbol{Q}_j}{dt} = \mathcal{L}_j\left(\boldsymbol{Q}, U\right), \tag{51a}$$

with

$$\mathcal{L}_j\left(\boldsymbol{Q}, U\right) = -\frac{1}{\Delta x}\left(\mathcal{A}^+\Delta\boldsymbol{Q}_{j-1/2} + \mathcal{A}^-\Delta\boldsymbol{Q}_{j+1/2} + \mathcal{A}\Delta\boldsymbol{Q}_j\right) + \boldsymbol{\Psi}_j\left(\boldsymbol{Q}, U\right), \tag{51b}$$

for $j = 1, 2, \ldots, N$. Here, $\boldsymbol{Q}$ and U are the vectors with components $\boldsymbol{Q}_j$ and U_j respectively, $\mathcal{A}^+\Delta\boldsymbol{Q}_{j-1/2}$ and $\mathcal{A}^-\Delta\boldsymbol{Q}_{j+1/2}$, are the right- and left-moving fluctuations, respectively, that are entering into the grid cell C_j, and $\mathcal{A}\Delta\boldsymbol{Q}_j$ is the total fluctuation within the cell. To determine these fluctuations, we need to solve Riemann problems (see below). Note that the term $\boldsymbol{\Psi}_j\left(\boldsymbol{Q}, U\right)$ in (51b) represents a discrete version of $\boldsymbol{\psi}$ over the grid cell C_j which can be evaluated straightforwardly by numerical differentiation techniques such as the finite-difference approximation of derivatives (cf. [29]).

Let us consider the fluctuations $\mathcal{A}^\pm\Delta\boldsymbol{Q}_{j-1/2}$ arising from the edge $(j-1/2)$ between cells C_{j-1} and C_j, for example. This amounts to solve the Cauchy problem for the homogeneous part of (50a) in the form :

$$\begin{cases} \boldsymbol{q}_t + \boldsymbol{f}\left(\boldsymbol{q}, u^L_{j-1/2}\right)_x = 0 & \text{if } x < x_{j-1/2} \\ \boldsymbol{q}_t + \boldsymbol{f}\left(\boldsymbol{q}, u^R_{j-1/2}\right)_x = 0 & \text{if } x > x_{j-1/2}, \end{cases} \tag{52a}$$

with the piecewise constant initial data at a given time t_0 :

$$\boldsymbol{q}\left(t_0, x\right) = \begin{cases} \boldsymbol{q}^L_{j-1/2} & \text{if } x < x_{j-1/2}, \\ \boldsymbol{q}^R_{j-1/2} & \text{if } x > x_{j-1/2}. \end{cases} \tag{52b}$$

Here $\boldsymbol{q}^L_{j-1/2} = \lim_{x\to x_{(j-1/2)^-}} \tilde{\boldsymbol{q}}_{j-1}(x)$ and $\boldsymbol{q}^R_{j-1/2} = \lim_{x\to x_{(j-1/2)^+}} \tilde{\boldsymbol{q}}_j(x)$ are the interpolated states obtained by taking limits of the reconstructed piecewise-continuous function $\tilde{\boldsymbol{q}}_{j-1}(x)$ or $\tilde{\boldsymbol{q}}_j(x)$ (each of them can be determined by applying a standard interpolation scheme to the set of discrete data $\{\boldsymbol{Q}_j(t_0)\}$, see [18, 28, 42] for more details) to the left and right of the cell edge at $x_{j-1/2}$, respectively. To find the set of interpolate states of $\{u^L_{j-1/2}\}$ and $\{u^R_{j-1/2}\}$, the approach we propose here is to solve the Helmholtz equation (50b) based on the the sets of data $\{\boldsymbol{q}^L_{j-1/2}\}$ and $\{\boldsymbol{q}^R_{j-1/2}\}$, respectively, which is a consistent approximation of u in the SGN model at the cell edges.

Note that if the conservative version of the flux $\boldsymbol{f}$ is being used in the problem formulation [32], the governing equation in the Riemann problem would be

$$\begin{cases} \boldsymbol{q}_t + \boldsymbol{f}\left(\boldsymbol{q}, u^L_{j-1/2}, (u_x)^L_{j-1/2}\right)_x = 0 & \text{if } x < x_{j-1/2} \\ \boldsymbol{q}_t + \boldsymbol{f}\left(\boldsymbol{q}, u^R_{j-1/2}, (u_x)^R_{j-1/2}\right)_x = 0 & \text{if } x > x_{j-1/2}. \end{cases}$$

Then it should be clear that the need to interpolate the set of states $\{(u_x)^L_{j-1/2}\}$ and $\{(u_x)^R_{j-1/2}\}$ consistently and to more than first-order accurate would complicate the matter further, and so it is preferable to use (50a) as the basis in the hyperbolic part of the method.

Here we are interested in the HLL (Harten, Lax, and van Leer) approximate solver [22] for the numerical resolution of the Riemann problem (52) where the basic structure of the solution is assumed to be composed of two discontinuities propagating at constant speeds $s^L_{j-1/2}$ and $s^R_{j-1/2}$ to the left and right, $s^L_{j-1/2} < s^R_{j-1/2}$, separating three constant states in the space-time domain. We assume that $s^L_{j-1/2}$ and $s^R_{j-1/2}$ are known a priori by some simple estimates based on the local information of the wave speeds (cf. [47, 32]). Then it is easy to find the constant state in the middle region, denoted by $q^*_{j-1/2}$, as

$$\boldsymbol{q}^*_{j-1/2} = \frac{s^R_{j-1/2}\boldsymbol{q}^R_{j-1/2} - s^L_{j-1/2}\boldsymbol{q}^L_{j-1/2} - \boldsymbol{f}(\boldsymbol{q}^R_{j-1/2}, u^R_{j-1/2}) + \boldsymbol{f}(\boldsymbol{q}^L_{j-1/2}, u^R_{j-1/2})}{s^R_{j-1/2} - s^L_{j-1/2}},$$

see [47] for more details. We then find the expression for the fluctuations in terms of jumps across each discontinuity :

$$\mathcal{A}^{\pm}\Delta\boldsymbol{Q}_{j-1/2} = \left(s^L_{j-1/2}\right)^{\pm}\left(\boldsymbol{q}^*_{j-1/2} - \boldsymbol{q}^L_{j-1/2}\right) + \left(s^R_{j-1/2}\right)^{\pm}\left(\boldsymbol{q}^R_{j-1/2} - \boldsymbol{q}^*_{j-1/2}\right), \tag{53}$$

where $s^+ = \max(s, 0)$ and $s^- = \min(s, 0)$.

Similarly, we can define fluctuation $\mathcal{A}\Delta\boldsymbol{Q}_j$ within cell C_j based on the solution of the following Riemann problem at the cell center x_j:

$$\begin{cases} \boldsymbol{q}_t + \boldsymbol{f}\left(\boldsymbol{q}, u^R_{j-1/2}\right)_x = 0 & \text{if } x < x_j \\ \boldsymbol{q}_t + \boldsymbol{f}\left(\boldsymbol{q}, u^L_{j+1/2}\right)_x = 0 & \text{if } x > x_j, \end{cases}$$

with the initial condition

$$\boldsymbol{q}\left(t_0, x\right) = \begin{cases} \boldsymbol{q}^R_{j-1/2} & \text{if } x < x_j \\ \boldsymbol{q}^L_{j+1/2} & \text{if } x > x_j. \end{cases}$$

To integrate the system of ODEs (51a) in time, we employ the strong stability-preserving (SSP) multistage Runge-Kutta scheme [21]. That is, in the first-order case we use the Euler forward time discretization as

$$\boldsymbol{Q}^{n+1}_j = \boldsymbol{Q}^n_j + \Delta t\mathcal{L}_j\left(\boldsymbol{Q}^n, U^n\right), \tag{54a}$$

where we start with the cell average $\boldsymbol{Q}^n_j \approx \boldsymbol{Q}_j(t_n)$ and $U^n \approx U(t_n)$ at time t_n, yielding the solution at the next time step $\boldsymbol{Q}^{n+1}_j$ over $\Delta t = t_{n+1} - t_n$. In the second-order case, however, we use the classical two-stage Heun method (also called the modified Euler method) as :

$$\begin{aligned} \boldsymbol{Q}^*_j &= \boldsymbol{Q}^n_j + \Delta t\mathcal{L}_j\left(\boldsymbol{Q}^n, U^n\right), \\ \boldsymbol{Q}^{n+1}_j &= \frac{1}{2}\boldsymbol{Q}^n_j + \frac{1}{2}\boldsymbol{Q}^*_j + \frac{1}{2}\Delta t\mathcal{L}_j\left(\boldsymbol{Q}^*, U^*\right). \end{aligned} \tag{54b}$$

It is common that the three-stage third-order scheme of the form

$$\begin{aligned} \boldsymbol{Q}^*_j &= \boldsymbol{Q}^n_j + \Delta t\mathcal{L}_j\left(\boldsymbol{Q}^n, U^n\right), \\ \boldsymbol{Q}^{**}_j &= \frac{3}{4}\boldsymbol{Q}^n_j + \frac{1}{4}\boldsymbol{Q}^*_j + \frac{1}{4}\Delta t\mathcal{L}_j\left(\boldsymbol{Q}^*, U^*\right), \\ \boldsymbol{Q}^{n+1}_j &= \frac{1}{3}\boldsymbol{Q}^n_j + \frac{2}{3}\boldsymbol{Q}^*_j + \frac{2}{3}\Delta t\mathcal{L}_j\left(\boldsymbol{Q}^{**}, U^{**}\right). \end{aligned} \tag{54c}$$

is a preferred one to be used in conjunction with the third- or fifth-order WENO (weighted essentially non-oscillatory) scheme that is employed for the reconstruction of $\tilde{\mathbf{q}}_j(x)$ during the spatial discretization (cf. [42]).

11.2 Numerical method for the elliptic step

To find the flow velocity u in SGN model at a given time t, the Helmholtz equation (50b) is solved with h and K known apriori, and subject to the prescribed boundary conditions (such as the Neumann and periodic boundaries considered here) at both ends. For simplicity, we use a three-point finite difference method on a uniform grid with mesh spacing Δx by first taking a backward difference for the outer derivative and then a forward difference for the inner derivative; collecting terms, we get the following constant coefficient difference formula for node j :

$$\alpha_j U_{j-1} + \beta_j U_j + \gamma_j U_{j-1} = K_j, \tag{55}$$

with α_j, β_j, and γ_j defined by

$$\begin{aligned}
\alpha_j &= -\frac{1}{3H_j}\frac{(H^3)_{j-1/2}}{(\Delta x)^2},\\
\beta_j &= \frac{1}{3H_j}\left(\frac{(H^3)_{j-1/2}}{(\Delta x)^2} + \frac{(H^3)_{j+1/2}}{(\Delta x)^2}\right) + 1,\\
\gamma_j &= -\frac{1}{3H_j}\frac{(H^3)_{j+1/2}}{(\Delta x)^2},
\end{aligned}$$

respectively, where $(H^3)_{j\pm1/2} = ((H_j)^3 + (H_{j\pm1})^3)/2 \approx (h(x_{j\pm1/2}, t))^3$ (cf. [29]). Going through all the nodal points for $j = 1, 2, \cdots, N$, and using the boundary conditions, we obtain a nonsingular linear system for the unknown velocity $U(t)$.

Let τ_j be the local truncation error of (55) to the Helmholtz equation (50b), *i.e.*,

$$\tau_j = \tilde{\alpha}_j u(t, x_{j-1}) + \tilde{\beta}_j u(t, x_j) + \tilde{\gamma}_j u(t, x_{j-1}) - K(t, x_j),$$

where

$$\begin{aligned}
\tilde{\alpha}_j &= -\frac{1}{3h(t, x_j)}\frac{h^3(t, x_{j-1/2})}{(\Delta x)^2},\\
\tilde{\beta}_j &= \frac{1}{3h(t, x_j)}\left(\frac{h^3(t, x_{j-1/2})}{(\Delta x)^2} + \frac{h^3(t, x_{j+1/2})}{(\Delta x)^2}\right) + 1,\\
\tilde{\gamma}_j &= -\frac{1}{3h(t, x_j)}\frac{h^3(t, x_{j+1/2})}{(\Delta x)^2}.
\end{aligned}$$

Then it is easy to show that τ_j is on the order of $(\Delta x)^2$, *i.e.*,

$$\tau_j = -\frac{(\Delta x)^2}{12h(t, x_j)}\left(\frac{1}{3}h^3(t, x_j)u_{xxxx}(t, x_j) + \frac{2}{3}h_x^3(t, x_j)u_{xxx}(t, x_j)\right) + O((\Delta x)^4), \tag{56}$$

and hence (55) is a second-order approximation to (50b) locally; the second-order global error of the method can be ensured, when the method remains stable, *i.e.*, the inverse of the martrix of the resulting linear system from the finite-difference approximation can be bounded by some constant independent of Δx, as $\Delta x \to 0$ (cf. [29]).

11.3 Numerical validation tests

To access the numerical accuracy that is attained by our method, we now perform a convergence study of the computed solutions for two benchmark tests where the exact solution are readily available for comparison. In all the runs considered here, the gravitational constant we take is $g = 10\ m/s^2$, and the Courant number is set to 0.5 for the stability of the hyperbolic solver.

11.3.1 Solitary wave problem

Our first test is the propagation of a single solitary wave in a periodic domain, where the analytic solution of the problem takes the form

$$h(t,x) = h_1 + (h_2 - h_1)\,\mathrm{sech}^2\left(\frac{(x - Dt)}{2}\sqrt{\frac{3(h_2 - h_1)}{h_2 h_1^2}}\right),$$

$$u(t,x) = D\left(1 - \frac{h_1}{h(t,x)}\right),$$

where h_1 denotes the layer depth at infinity, h_2 denotes under a wave crest, and D denotes the speed of the wave that is related to h_2 by $D = \sqrt{gh_2}$ (cf. [32]). In the numerical experiments considered below, the quantities we take are $h_1 = 10\ m$ and $h_2 = 22.5\ m$, yielding $D = 15\ m/s$; the computational domain is of size 300 m with periodic boundary conditions at both ends.

Table 1 shows 1-norm errors of the height at time $t = 40\ s$ (time it takes the solitary wave crest to travel one period) for a convergence study of the solutions obtained using our numerical strategy with four different mesh sizes $N = 1200$, 2400, 4800, and 9600, and three different hyperbolic integration schemes. The underlying Helmholtz solver for (55) is the second-order finite difference scheme.

Let $E^1(h) = \{E_j^1(h)\}$ for $j = 1, 2, 3, 4$ be the sequence of the 1-norm error of the computed water height h to its true solution on an $N = \{1200, 2400, 4800, 9600\}$ grid. With that, it is a common practice to estimate the rate of convergence using the errors on two consecutive grids based on the formula

$$\text{convergence order} = \frac{\ln\left(E_{j-1}^1(h)/E_j^1(h)\right)}{\ln\left(N_{j-1}/N_j\right)}.$$

From Table 1, we observe that when Godunov method is employed in the hyperbolic step, (*i.e.*, the method uses zeroth-order piecewise constant reconstruction scheme for the Riemann data at the cell edges, and the forward Euler method (54a) for the time discretization), the order of accuracy of algorithm approaches to first-order accurate as the mesh is refined, and it is second-order accurate, when MUSCL (monotonic upstream-centered scheme for conservation laws) is employed alternatively (*i.e.*, both the first-order piecewise linear reconstruction scheme and the Heun method (54b) are in use). In the WENO 3 case, however, (*i.e.*, the method uses the third-order WENO (weighted essentially non-oscillatory) scheme for Riemann data reconstruction, and the third-order method (54c) for the time discretization), the order of accuracy in average is 2.1 approximately which is less than 3 (the formal order of accuracy of the hyperbolic solver WENO 3); this result may not come as a surprise because our underlying Helmholtz solver is only of $O((\Delta x)^2)$. Nevertheless, among all the three methods, WENO 3 gives the smallest error in magnitude for each mesh size.

It should be mentioned that by following the approach proposed by Britti *et al.* [3], a fourth-order compact Helmholtz solver can be derised by eliminating the terms that contain u_{xxx} and

Table 1: Numerical results for the solitary wave problem obtained using our algorithm with four different mesh sizes and three different hyperbolic integration schemes; 1-norm errors in the height are shown at time $t = 40$s. The Helmholtz equation (55) is solved using second-order finite difference scheme in all cases.

Hyperbolic step	Godunov		MUSCL		WENO 3	
N	$E^1(h)$	order	$E^1(h)$	order	$E^1(h)$	order
1200	2.595e+02		4.894e+00		2.622e−01	
2400	1.470e+02	0.82	1.210e+00	2.02	4.410e−02	2.57
4800	7.834e+01	0.91	3.005e−01	2.01	1.178e−02	1.90
9600	4.044e+01	0.95	7.487e−02	2.01	3.060e−03	1.94

Table 2: Numerical results for the periodic travelling wave problem; 1-norm errors in the height are shown at the time where the wave travelled over four periodic distance of the domain.

Hyperbolic step	Godunov		MUSCL		WENO 3	
N	$E^1(h)$	order	$E^1(h)$	order	$E^1(h)$	order
300	1.346e−01		5.250e−03		3.521e−03	
600	7.749e−02	0.83	1.094e−03	2.37	4.563e−04	3.09
1200	4.100e−02	0.92	2.482e−04	2.15	5.927e−05	2.96
2400	2.112e−02	0.96	6.072e−05	2.03	7.923e−06	2.90

u_{xxxx} on the right-hand size of the local truncation error (56). But since doing so would involve additional approximation of derivatives such as h_x, h_{xx}, K_x, and K_{xx}, to keep the basic idea of the algorithm simple, it will not be discussed further.

11.3.2 Travelling wave problem

Our second example concerns the propagation of a travelling wave in a periodic domain of one wave length. In this case, the exact solution of the water height written in terms of the Jacobi elliptic function follows (17), and the velocity is determind from (13). The water heights we take in the computations are $h_0 = 1.0962\ m$, $h_1 = 1.1\ m$, and $h_2 = 1.2\ m$, yielding the wave speed $D \approx 3.36413$ m/s and wave length $\lambda \approx 26.3767\ m$; the computational domain is of size of one wave length with periodic boundary conditions at both ends.

As in Section 11.3.1, a convergence study of the solution is performed, and the results are shown in Table 2. From the table, we observe similar rate of convergence as in Table 1, when the Godunov and the MUSCL methods are in used in the hyperbolic step of the algorithm, and a slightly better behavior of error when WENO 3 is employed.

11.3.3 Dam-break problem

We now present numerical results to the simulation of a dam-break problem studied in [7, 32, 36], for instance. Since there is no analytical solution to this problem, such a study is rather qualitative, but

it allows us to recover some qualitative characteristics of the solution (the amplitude of the leading wave and its velocity, for example). We take the velocity vanishing in the entire computational domain of size $x \in [-300, 300]$ m, $u(0,x) = 0$ m/s, while the water depth is piece-wise constant :

$$h(0,x) = \begin{cases} h_L, & \text{if } x < 0, \\ h_R, & \text{if } x \geq 0, \end{cases}$$

where h_L and h_R are chosen to be 1.8 m and 1 m, respectively.

The discontinuous initial data for the water depth will be replaced by a smooth function :

$$h(0,x) = h_R + \frac{h_L - h_R}{2}\left(1 - \tanh\left(\frac{x}{\alpha}\right)\right), \tag{57}$$

where $\alpha = 2$ m or $\alpha = 0.4$ m. The structure of the solution (but not the velocity of the leading solitary wave and its velocity) depends on the value of α. According to the terminology given in [36], the case $\alpha = 2$ m produces S_2 configuration (flat structure of the fluid depth behind the dispersive shock, Figure 14), while $\alpha = 0.4$ m produces S_3 configuration (existence of a node type point in the fluid depth profile, Figure 15). The node point moves with the velocity which can be estimated by using the continuity through dispersive shock of the Riemann invariant to the Saint-Venant equations corresponding to right facing waves.

The comparison of the analytical and numerical results for the amplitude of the leading solitary wave is shown in Fig. 14 and 15 at time $t = 47.434$ s with the mesh size $\Delta x = 0.025$ m (*i.e.*, $N = 24000$ meshes).

We also note that as far as the global wave structure is concerned, our results are in good agreement with the ones shown in [7] at time $t = 150$ s, where a different gravitational constant, *i.e.*, $g = 1$ m/s^2, is employed there.

Here the computation was carried out using our algorithm with the WENO 3 scheme in the hyperbolic part, and the second-order finite difference method in the elliptic part. Non-reflecting boundary condition is used on the left and right boundaries during the computations.

12 Conclusion

We study the inertia type regularization of hyperbolic systems of equations. The Serre-Green-Naghdi equations describing surface gravity waves in shallow water are used for the corresponding numerical applications.

We show that the inertia type dispersive terms are not always regularizing. The solution can develop shocks which relate a constant state and periodic wave train. These shocks are quite specific. First, the shock speed coincides necessarily with the phase velocity of the corresponding wave train. Second, the associated jump conditions are nothing more than the Rankine-Hugoniot relations for the corresponding Whitham equations (modulation equations).

The numerical evidence of such shocks is provided. This phenomena is quite stable, such shocks appear even in the case of linearized inertia type dispersion.

Acknowledgments Parts of this research were conducted during a visit of SG and BN to the Department of Mathematics of National Taiwan University. SG was partially supported by l'Agence Nationale de la Recherche, France (grant numbers ANR-11-LABEX-0092, and ANR-11-IDEX-0001-02). KMS was partially supported by MOST 105-2115-M-002-013-MY2.

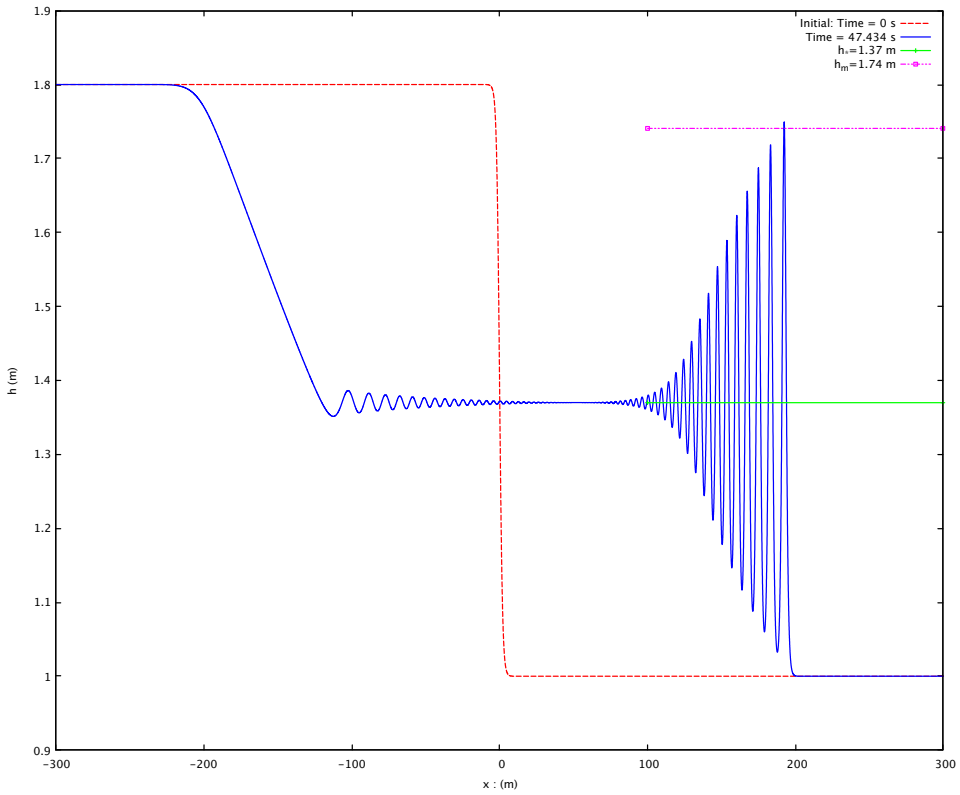

Figure 14: Numerical result for the dam-break problem for the initial data (57) with $\alpha = 2\ m$ (S_2 case in the terminology of [36]). The solid line is the water depth at time $t = 47.434$s, and the dashed line is the initial condition. The lines for h_* and h_m are the depths of the post right-going undular bore and the leading solitary wave (cf. [7]), respectively.

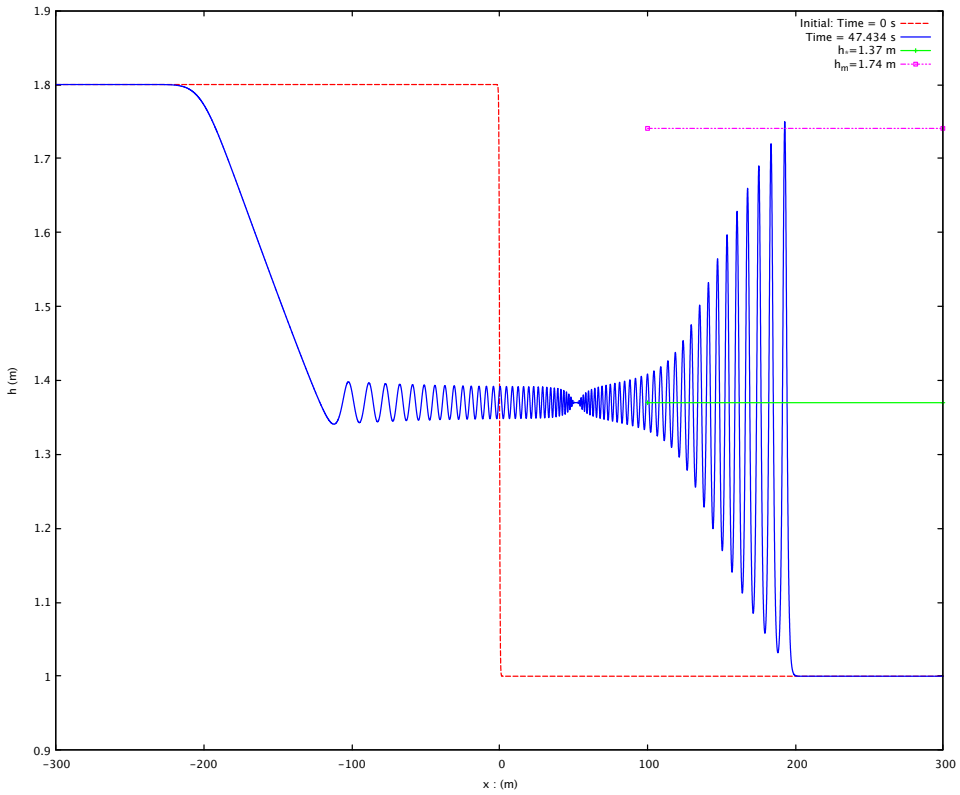

Figure 15: Numerical result for the dam-break problem for the initial data (57) with $\alpha = 0.4\ m$ (S_3 case in the terminology of [36]). The solid line is the water depth at time $t = 47.434$s, and the dashed line is the initial condition. The lines for h_* and h_m are the depths of the post right-going undular bore and the leading solitary wave (cf. [7]), respectively.

References

[1] M. A. Ablowitz, G. Biondini, I. Rumanov, Whitham modulation theory for (2+1)-dimensional equations of Kadomtsev-Petviashvili type, Phys. A: Math. Theor. in press https://doi.org/10.1088/1751-8121/aabbb3

[2] V. Berdichevsky, *Variational Principles of Continuum Mechanics, I. Fundamentals*, Springer, 2009.

[3] S. Britt, S. Tsynkov, and E. Turkel. A compact fourth order scheme for the Helmholtz equation in polar coordinates. *J. Sci. Comput.*, 45:26–47, 2010.

[4] D. Clamond, D. Dutykh, D. Mitsotakis, Conservative modified Serre–Green–Naghdi equations with improved dispersion characteristics, Commun. Nonlinear Sci. Numer. Simulat. **45** (2017) 245–257.

[5] F. Dias, P. Milewski, On the fully-nonlinear shallow-water generalized Serre equations, Phys. Lett. A **374** (2010), 1049–1053.

[6] G. A. El, V. V. Geogjaev, A. V. Gurevich, A. L. Krylov, Decay of an initial discontinuity in the defocusing NLS hydrodynamics, Physica D: Nonlinear Phenomena **87**(1995) 186–192.

[7] G.A. El, R.H.J. Grimshaw and N.F. Smyth, Unsteady undular bores in fully nonlinear shallow-water theory, Phys. Fluids **18** (2006), 027104.

[8] G. A. El, M. Hoefer, Dispersive shock waves and modulation theory, Physica D, **333** (2016) 11-65.

[9] G. A. El, M. A. Hoefer, M. Shearer, Expansion shock waves in regularized shallow water theory, Proc. Royal Soc. A **472** (2016).

[10] N. Favrie, S. Gavrilyuk, A rapid numerical method for solving Serre-Green-Naghdi equations describing long free surface gravity waves, Nonlinearity 30 (7) (2017).

[11] S. Gavrilyuk, Large amplitude oscillations and their 'thermodynamics' for continua with 'memory', European Journal of Mechanics B/ Fluids, **13** (6)(1994), 753-764.

[12] S. Gavrilyuk, D. Serre, A model of a plug-chain system near the thermodynamic critical point: connection with the Korteweg theory of capillarity and modulation equations, 419-428, in book : IUTAM Symposium on Waves in Liquid/Gas and Liquid/Vapor Two-Phase Systems, Eds. S. Morioka and L. van Wijngaarden, Kluwer Academic Publishers, 1995.

[13] S. Gavrilyuk and V. Teshukov, Generalized vorticity for bubbly liquid and dispersive shallow water equations, Continuum Mechanics and Thermodynamics **13** (2001), 365–382.

[14] S. Gavrilyuk, H. Kalisch and Z. Khorsand A kinematic conservation law in free surface flow, Nonlinearity, **13** (2015) 1805–1821.

[15] S. Gavrilyuk, Multiphase Flow Modeling via Hamilton's principle. In : Variational Models and Methods in Solid and Fluid Mechanics, CISM Courses and Lectures, v. 535 (Eds. F. dell'Isola and S. Gavrilyuk), Springer, 2011.

[16] A.E. Green, N. Laws, and P.M. Naghdi, On the theory of water waves, Proc. R. Soc. Lond. **A 338** (1974), 43–55.

[17] A. E. Green and P. M. Naghdi, A derivation of equations for wave propagation in water of variable depth, J. Fluid Mech. **78** (1976), 237–246.

[18] E. Godlewski and P.-A. Raviart, Numerical Approximation of Hyperbolic Systems of Conservation Laws, Applied Mathematical Science 118, Springer-Verlag, 1996.

[19] A. Gurevich, L. Pitaevskii, Nonstationary structure of a collisionless shock wave, JETP **38**, 291 - 297 (1974).

[20] A. V. Gurevich, A. L. Krylov, Dissipationless shock waves in media with positive dispersion, Zh. Eksp. Teor. Fiz. **92**(1987) 1684–1699.

[21] S. Gottlieb, C.-W. Shu, and E. Tadmor. Strong stability preserving high-order time discretization methods. *SIAM Review*, 43:89–112, 2001.

[22] A. Harten, P.D. Lax, B. van Leer, On upstream differencing and Godunov-type schemes for hyperbolic conservation laws. SIAM Review **25**, 35–61 (1983).

[23] T. Y. Hou and P. D. Lax, Dispersive approximations in fluid mechanics, Communications on Pure and Applied Mathematics, **44**(1) (1991), 1–40.

[24] A. M. Kamchatnov, Nonlinear Periodic Waves and Their Modulations: An Introductory Course, World Scinetific Publishing, 2000.

[25] D. I. Ketcheson and R. J. LeVeque, WENOCLAW: A higher order wave propagation method, in: Hyperbolic Problems: Theory, Numerics, Applications, Springer-Verlag, 2008, 609–616.

[26] D. I. Ketcheson, M. Parsani, and R. J. LeVeque, High-order wave propagation algorithm for hyperbolic systems, SIAM J. Sci. Comput., **35(1)**(2013), A351–A377.

[27] D. Lannes, The Water Waves Problem. Mathematical Surveys and Monographs, vol. **188** (Amer. Math. Soc., Providence, 2013).

[28] R. J. LeVeque, Finite Volume Methods for Hyperbolic Problems, Cambridge University Press, 2002.

[29] R. J. LeVeque, Finite Difference Methods for Ordinary and Partial Differential Equations: Steady-State and Time-Dependent Problems, SIAM, Philadelphia, 2007.

[30] M. Li, P. Guyenne, F. Li and L. Xu, High order well-balanced CDG-FE methods for shallow water waves by a Green-Naghdi model, J. Comp. Physics **257** (2014), 169–192.

[31] N. Makarenko, A second long-wave approximation in the Cauchy-Poisson problem, Dynamics of Continuous Media, v. 77 (1986), pp. 56-72 (in Russian).

[32] O. Le Métayer, S. Gavrilyuk, and S. Hank, A numerical scheme for the Green-Naghdi model, J. Comp. Phys. **229** (2010), 2034–2045.

[33] J. von Neumann, Proposal and analysis of a numerical method for the treatement of hydrodynamical shock problems, Off. Scient. Res. and Dev. Report. OSRD-3617 (1944)

[34] J. Miles and R. Salmon, Weakly dispersive nonlinear gravity waves, J. Fluid Mechanics **157** (1985), 519–531.

[35] M. Pavlov, Nonlinear Schrödinger equation and the Bogolyubov-Whitham method of averaging, Teoreticheskaya Matematicheskaya Fizika **71**(1987) 351–356.

[36] J.P.A. Pitti, C. Zoppou, and S.G. Roberts, Behaviour of the Serre equations in the presence of steep gradients revisited, arXiv:1706.08637v1 [math NA] 27 Jun 2017.

[37] J. W. S. Rayleigh, On the theory of surface forces–II. Compressible fluids. Phil. Mag. **33** (1892) 209–220.

[38] J. W. S. Rayleigh, The theory of sound, V. 1. Dover Publications, New York (1945).

[39] J.-C. Saut and L. Xu, Well-posedness on large time for a modified full dispersion system of surface waves. J. Math. Phys. **53** (2012), 115606, 12 pp.

[40] F. Serre, Contribution à l'étude des écoulements permanents et variables dans les canaux, La Houille Blanche **8** (1953), 374–388.

[41] D. Serre, Systèmes de lois de conservation (I), Diderot, 1996.

[42] C.-W. Shu, High order weighted essentially nonoscillatory schemes for convection dominated problems, SIAM Review, **5** (2009), 82–126.

[43] K.-M. Shyue and F. Xiao, An Eulerian interface sharpening algorithm for compressible two-phase flow: The algebraic THINC approach, J. Comput. Phys., **268** (2014), 326–354.

[44] M. Slemrod, 1983, Admissibility criteria for propagating phase boundaries in a van der Waals fluid, Archive Rat. Mech. Anal. **81**, 301–315.

[45] O. Steinbach, Numerical Approximation Methods for Elliptic Boundary Value Problems: Finite and Boundary Elements, Springer, 2007.

[46] C. H. Su, C. S. Gardner, Korteweg - de Vries Equation and Generalisations. III. Derivation of the Korteweg - de Vries Equation and Burgers Equation, J. Math. Physics, **10** (1969) 536–539.

[47] E. F. Toro, Riemann Solvers and Numerical Methods for Fluid Dynamics, Springer-Verlag, Berlin, Heidelberg, 1997.

[48] L. Truskinovsky, Equilibrium phase boundaries, Sov. Phys. Dokl. **27** (1982) 551–553.

[49] L. Truskinovsky, Critical nuclei in the van der Waals model, Sov. Phys. Dokl. **28** (1983) 248–250.

[50] L. Truskinovsky, Dynamics of nonequilibrium phase boundaries in a heat conducting nonlinear elastic medium, J. Appl. Math. Mech. (PMM), **51** (1987) 777–787.

[51] J. D. Van der Waals, 1893 The thermodynamic theory of capillarity under the hypothesis of a continuous density variation. Transl. J. S. Rowlinson, J. Stat. Physics, **20,** 197–244 (1979).

[52] G. B. Whitham, Linear and Nonlinear Waves, John Wiley and Sons, 1974.